CONSTRUCTION AND CHARACTERIZATION OF REMOVABLE AND REUSABLE PIEZOELECTRIC ACTUATORS

by

Thomas Wade McCray

Thesis submitted to the Faculty of Virginia Polytechnic Institute and State University in partial fulfillment of the requirements for the degree of

MASTER OF SCIENCE

in Mechanical Engineering

APPROVED:

Harley H Cudney

Dr. H.H. Cudney, Chair

Dr. A.L. Wicks

Dr. H.H. Robertshaw

CONSTRUCTION AND CHARACTERIZATION OF REMOVABLE AND REUSABLE PIEZOELECTRIC ACTUATORS

by

Thomas W. McCray

Committee Chair: Harley H. Cudney

Department: Mechanical Engineering

Abstract

Piezoelectric patch-type actuators are being considered for use in acoustic control and vibration control of complex mechanical structures such as aircraft fuselages and automobile interiors. For complex structures, it is often difficult to predict the best location of actuator-structure interaction. Currently, piezoelectric patch-type actuators are bonded permanently to the host structure using a technique that requires surface preparation. This technique is not well suited for actuator performance testing and model verification since attaching the actuator is time consuming, removing the actuator is difficult, and the actuator is destroyed when it is removed.

We present three alternate techniques for bonding flat piezoelectric patch-type actuators to structures. These techniques allow the actuator to be attached quickly, removed easily, and reused. The alternate techniques and a permanent bonding technique are used to

attach actuators to a clamped-free beam. For each attachment technique, we obtain the frequency response functions, actuator authority levels, and damping ratios. We also obtain the degradation of the actuator authority and damping ratio as the actuator is reused. For each attachment technique, we compare the measured performance to the performance predicted from a pin-force model of that actuator attachment.

The attachment techniques that allowed us to make removable, reusable piezoelectric actuators were shown to provide structural actuation very similar to actuation provided by permanently attached piezoelectric actuators. A small but statistically significant change in authority occurred as a result of removing the actuator. The confidence intervals of actuator authority increased in frequency regions of antiresonance and closely spaced modes. The pin-force model did not provide an accurate analysis method for predicting actuator authority.

Acknowledgments

Although much work is performed by the master's candidate, a master's thesis is a task that requires more than one person; therefore, thanks to several persons are in order. I would like to thank my advisor, Dr. Harley Cudney, for providing insight to my research as well as his sincere interest and advice in my future career in engineering. I also want to thank my committee, Dr. Harry Robertshaw and Dr. Al Wicks, for providing me with questions and comments that have stretched my knowledge of science, engineering, and mathematics. I would also like to thank my labmates Anton Sumali, Rich Lomenzo, Jon Hill, Wes Holley, and David Schmiel for their day to day humor, help and support in the lab.

I would like to thank the mechanical engineering faculty of Virginia Polytechnic Institute and State University for the excellent education that I have received. In addition to this, I would like to thank the mechanical engineering department for the assistantship funding that I have received and needed to complete my education at Virginia Tech.

I would like to thank my parents, family, and friends for their shared excitement and support of my graduate education. Finally and most importantly, I would like to thank God for giving me a mind with which I can think and reason and accomplish a task such as this.

Table of Contents

List of Figures

List of Tables

Nomenclature

Roman Letters

A	cross sectional area
b	width of beam
C	matrix containing the coefficients of a linear, least squares curve fit
$c_{1,2}$	coefficients of a linear, least squares curve fit
d	distance from centroid of a material layer to the neutral axis
E	elastic modulus
F	force
I	moment of inertia
M	bending moment
n	ratio of one elastic modulus to another
N	number of samples
s	sample standard deviation
t	Student' t value, thickness
$\hat{u}$	estimated parameter value
U	column vector containing sample values
x	individual sample value
$\bar{x}$	sample mean
X	matrix containing ones in the first column and sample values in the second column
$\frac{Xk}{F_0}$	non dimensional frequency response function magnitude

y	distance from neutral axis to a point on the structure
$\bar{y}$	distance from the centroid of a material layer to the centroid of the cantilevered beam
$\bar{Y}$	distance from the centroid of the cantilevered beam to the neutral axis

Greek Letters

ε	strain
Λ	induced strain
μ	population mean
ρ	radius of curvature
σ	stress
ω	excitation frequency
ω_n	natural frequency
ψ	ratio of thickness and elastic modulus of one material to another
ζ	damping ratio

Subscripts

a	piezoelectric actuator
ax	axial
b	bending
i	sample number, material layer
s	host structure
tot	total

x	individual parameter
$\alpha/2$	confidence ratio

CHAPTER 1
INTRODUCTION

1.1 Current Uses of Piezoelectric Actuators

In order to understand the content of this research, it is beneficial to know the current uses and applications of piezoelectric actuators. There are several applications of piezoelectric actuators in the area of structural vibration and acoustic control. Using piezoelectric actuators as control devices can significantly reduce the structural vibration of cantilevered beams and simply supported plates. Research in this area has been conducted in order to observe the performance of piezoelectric actuators. The results of one research project indicated significant vibration reduction of an aluminum plate by the use of a single piezoelectric actuator (D'Cruz, 1993). In another research project, Hollkamp theoretically and experimentally verified multimodal vibration suppression of a cantilevered beam (1994). In his work, he designed a resonant-shunted piezoelectric actuator that controlled the second and third bending modes of a cantilevered beam.

In addition to these findings, several researchers have applied optimization techniques and placement procedures to the uses and applications of piezoelectric actuators. Optimal piezoelectric actuator placement for up to three piezoelectric actuators on a plate structure was accomplished by Wang, Fuller, and Burdisso (1994). Also, optimal vibration control procedures for a cantilevered beam were designed by Hanagud *et al.* (1992).

The previous applications of piezoelectric actuators involved simple structures such as cantilevered beams and simply supported plates; however, piezoelectric actuators are also being used to control vibration and acoustic responses of structures that are more complex. The following examples describe the complex structures as well as the manner in which the piezoelectric actuators were attached. Global acoustic attenuation of a homogeneous cylindrical shell has been accomplished using piezoelectric actuators (Fuller, 1992). The piezoelectric actuators in the experimental apparatus were adhesively bonded to the surface of the cylinder, and the actuation was through the length and width of the piezoelectric actuator. Rotor bearing vibration has also been reduced through the use of piezoelectric actuators (Palazzolo, 1993). The actuators used in this case were a system of stacked piezoelectric actuators acting through their thickness. Actuators of this type are enclosed in a housing that can be inserted and removed from the host structure without an adhesive material.

Typically, there are two methods of attaching piezoelectric actuators to their host structure. They can be bonded to the surface of the structure as in Fuller's work. They can also be stacked together and enclosed in a casing that is then attached to the host structure as in Palazzolo's work. The piezoelectric actuators that are bonded to the surface are generally bonded with a high strength, permanent bond adhesive. Due to its brittleness, the piezoelectric actuator generally cannot be removed from the host structure once the adhesive has been used; however, there are certain instances when removing a piezoelectric actuator from its host structure would be beneficial. For structures where the best location of a piezoelectric actuator is not apparent, several tests would need to be performed in order to determine the best location. Unless a removable, reusable actuator

was used, experimental testing would require permanently bonding a piezoelectric actuator to each location of interest.

1.2 Objective

A plausible solution to this problem would be to construct a removable and reusable actuator that would allow testing of the structure in several locations without permanently attaching an actuator. The objective of this research is to develop and construct three alternate techniques for bonding flat piezoelectric patch-type actuators to structures. These techniques will allow the actuator to be attached quickly, removed easily, and reused. The alternate techniques and the permanent bonding technique will be used to attach actuators to a clamped-free beam. For each attachment technique, the frequency response function, actuator authority, and damping ratio will be obtained as well as their degradation over several removals from the host structure. For each attachment technique, comparisons of the measured performance to the performance predicted from a pin-force model of that actuator attachment will be made.

1.3 Approach

Currently, there is no previous work in the area of removable reusable piezoelectric actuators; therefore, some different methods of constructing such an actuator should be considered. There are several methods of structure actuation, and, likewise, there are several potential methods for estimating the performance of a piezoelectric actuator. For example, an electromagnetic shaker could be used to actuate a structure, and from that information, the experimentalist could predict the piezoelectric actuator performance.

However, the interaction between an electromagnetic shaker with a structure is quite different from the interaction between a piezoelectric actuator with the same structure. The frequency response functions between a shaker and a cantilevered beam and a permanently attached piezoelectric actuator and a cantilever beam are illustrated and discussed in Chapter 5. It is shown that there is a significant mismatch between the modes and antiresonances of the shaker and piezoelectric actuator frequency response functions. This mismatch is particularly dangerous if one of the missing modes was to be controlled by the permanently attached actuator. An actuator that has similar response characteristics to the piezoelectric actuator would be more suitable in predicting the performance characteristics of the permanent actuator before it is attached. A solution to this problem would be to use a similar piezoelectric actuator as the testing device. The following paragraph describes in detail the three attachment techniques that are used in this research.

The construction of a removable, reusable piezoelectric patch-type actuator first involves attaching the piezoelectric patch to another structure of similar area and stiffness. This combination of an actuator and stiffener would then be attached to the host structure. The piezoelectric actuator will have to actuate through the stiffener before having an effect on the host structure. The stiffener will provide stiffness to the piezoelectric actuator so that the actuator system can be removed without damaging the brittle piezoelectric actuator. Figure 1.1 illustrates the construction of the permanent attachment technique and each removable, reusable attachment technique. The first removable, reusable attachment technique involves a piezoelectric actuator that is cemented to an aluminum stiffener and then cemented the stiffener to the beam. The second attachment technique involves a piezoelectric actuator that is cemented to an aluminum stiffener and then attached the

stiffener to the beam with wax. The third attachment technique involves a piezoelectric actuator that is attached to the beam only with wax.

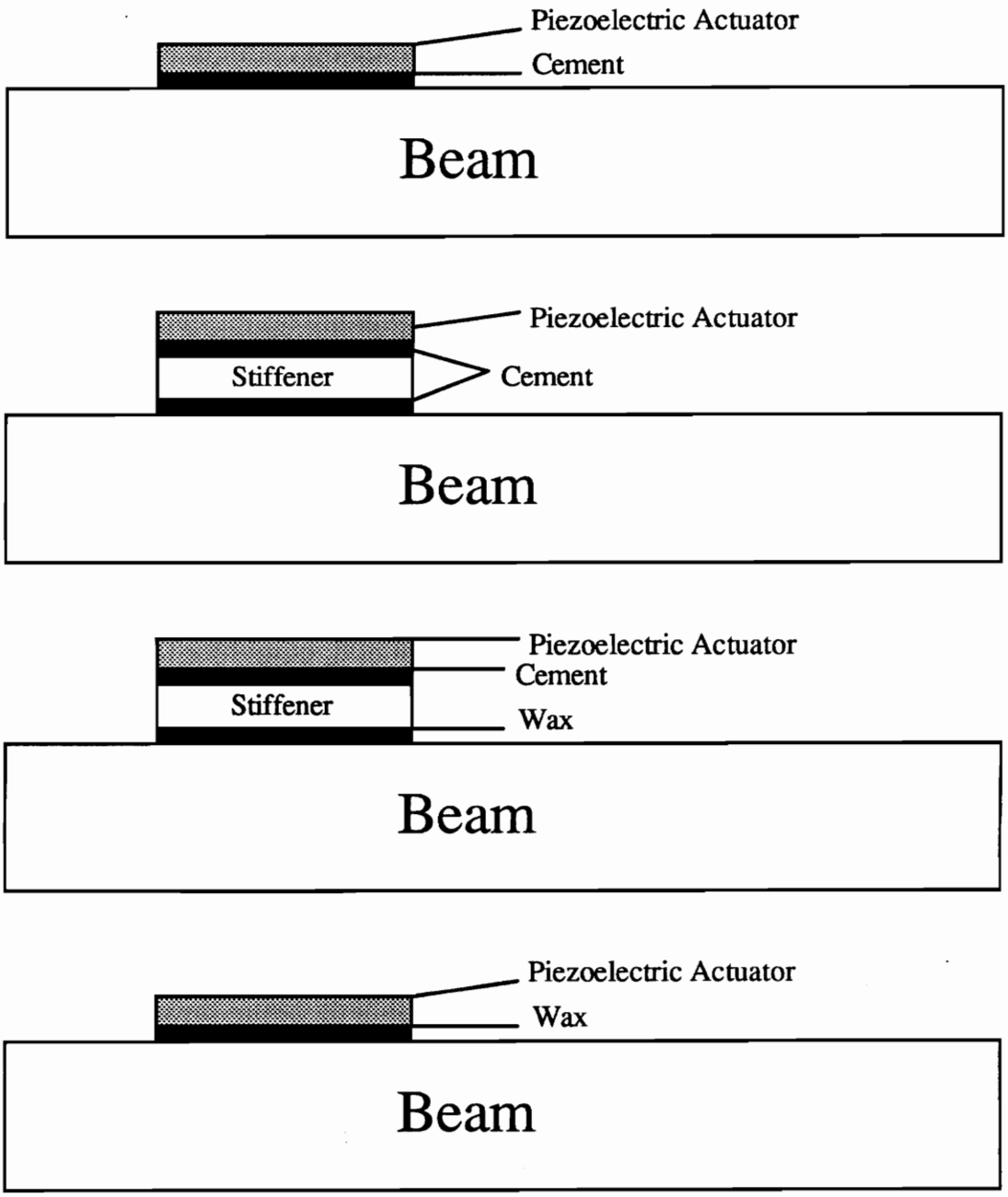

Figure 1.1. Actuator Attachment Techniques

Removal of the actuators can be accomplished as follows. The first removable, reusable actuator will be removed by prying the stiffener away from the beam until the cement bond is broken. Considerable deformation to the piezoelectric actuator will result in this removal technique. The second actuator, attached to the beam with a stiffener and wax, will be removed by pushing the actuator at the stiffener until it can be lifted off the beam. An insignificant amount of deformation will be involved in this removal technique. The third actuator will be removed by heating the actuator until the wax is soft enough to remove the actuator by hand. Like the previous case, this will involve insignificant deformation to the piezoelectric actuator.

In order to characterize the influence of the removable, reusable actuators, both theoretical calculations and experimental tests will be conducted. The theoretical calculations will involve calculating the bending moment supplied to the beam by the piezoelectric actuator. The bending moment will be calculated for each attachment technique. The experimental tests will involve obtaining the frequency response function and coherence function between the input voltage to the piezoelectric actuator and the tip acceleration of the clamped-free beam. The frequency response function and coherence function will likewise be obtained for each attachment technique.

1.4 Outline

Chapter two will begin with a review of the pin-force model. This modeling technique will then be applied to one piezoelectric actuator that is attached to a beam with several bonding layers. Chapter three includes an outline and discussion of the dynamic response characteristics of the removable, reusable piezoelectric actuators. A discussion of the

experimental design is included in chapter four, and the results and observations of the experiments and theoretical calculations will follow in chapter five. Finally in chapter six, conclusions about the research will be stated.

CHAPTER 2
PRESENTATION OF THE PIN-FORCE MODEL

The axial force and bending moment supplied by piezoelectric patch-type actuators on beams can be predicted from the pin-force model, introduced by Lazarus and Crawley, (1989). In this model of the piezoelectric actuator and host structure system, the piezoelectric actuator is considered to exert a force on the host structure through "pin connections" at the edges of the actuator. In this chapter we will first review the pin-force model of a beam excited by two piezoelectric actuators mounted symmetrically with respect to the neutral axis of the beam. This modelling technique will be used to model the axial force and bending moment created by a single actuator rather than a pair of actuators. The effects of several bonding layers on the resulting axial force and bending moment will then be included in the model. This will give us a tool from which to predict the authority of the beam due to actuators mounted with each attachment technique.

2.1 Axial Force, Two Piezoelectric Actuators

Figure 2.1 illustrates the free-body diagram of an elastic beam and two piezoelectric actuators excited with the same magnitude and in phase with one another. A perfect bonding layer is assumed to exist between the piezoelectric actuators and beam. The perfect bonding layer assumption means that the shear stress between the piezoelectric actuator and the beam is localized at the ends of the piezoelectric actuator. These ends are modelled as pin connections. The induced strains of the piezoelectric actuators will cause axial forces to occur at the pin connections. The resulting action on the beam is an

axial force acting through its neutral axis that is twice the magnitude of one actuator acting by itself. The moments at the neutral axis produced by pin forces acting at the surface of the beam are equal in magnitude but opposite in sense; therefore, they cancel each other.

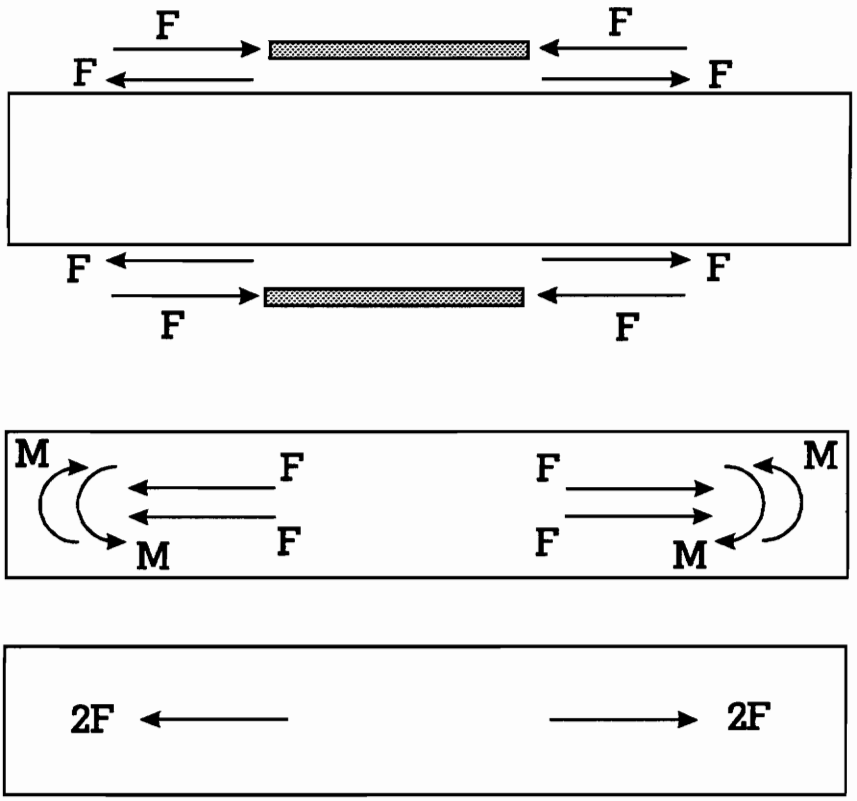

Figure 2.1. Axial Force Produced by Two Piezoelectric Actuators

Due to the axial force, the strain throughout the thickness of the beam will be assumed to be constant. Since stress is proportional to strain according to Hooke's Law, the stress throughout the thickness of the beam will also be constant (see Figure 2.2).

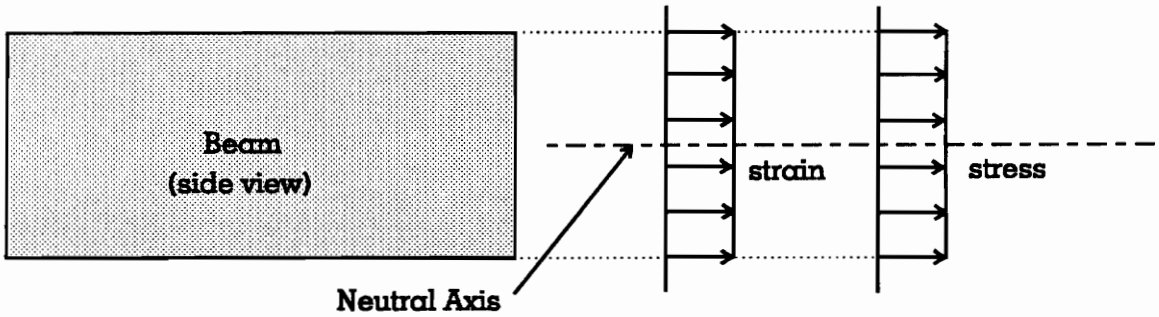

Figure 2.2. Strain and Stress Profile of the Structure

From the previous information, the equation for the axial force acting through the beam can be derived. The equation for the axial force, adapted from Crawley's work, that is acting through the beam normalized with respect to its width is

$$\frac{F_{tot}}{b} = \Lambda E_s t_s \left(\frac{2}{2+\psi} \right) \tag{1}$$

where F_{tot} is the total force acting through the structure, b is the width of the structure, and Λ denotes the induced strain of the piezoelectric actuator. The non-dimensional parameter, ψ, is given as follows,

$$\psi = \frac{E_s t_s}{E_a t_a} \tag{2}$$

where E_s is the elastic modulus of the structure, t_s is the thickness of the structure, E_a is the elastic modulus of the piezoelectric actuator, and t_a is the thickness of the piezoelectric actuator.

2.2 Bending Moment, Two Piezoelectric Actuators

Figure 2.3 illustrates the free-body diagram of a beam and two piezoelectric actuators excited out of phase with one another. As in the previous case, a perfect bonding layer between the beam and piezoelectric actuator is assumed to exist. The induced strains of the piezoelectric actuators will result in forces at the pin connections that are equal in magnitude but opposite in sense. The extension force of one piezoelectric actuator will cancel the compressive force of the other piezoelectric actuator. The couples produced by the piezoelectric actuators, however, add together to produce a bending moment that is twice the value of one piezoelectric actuator acting by itself.

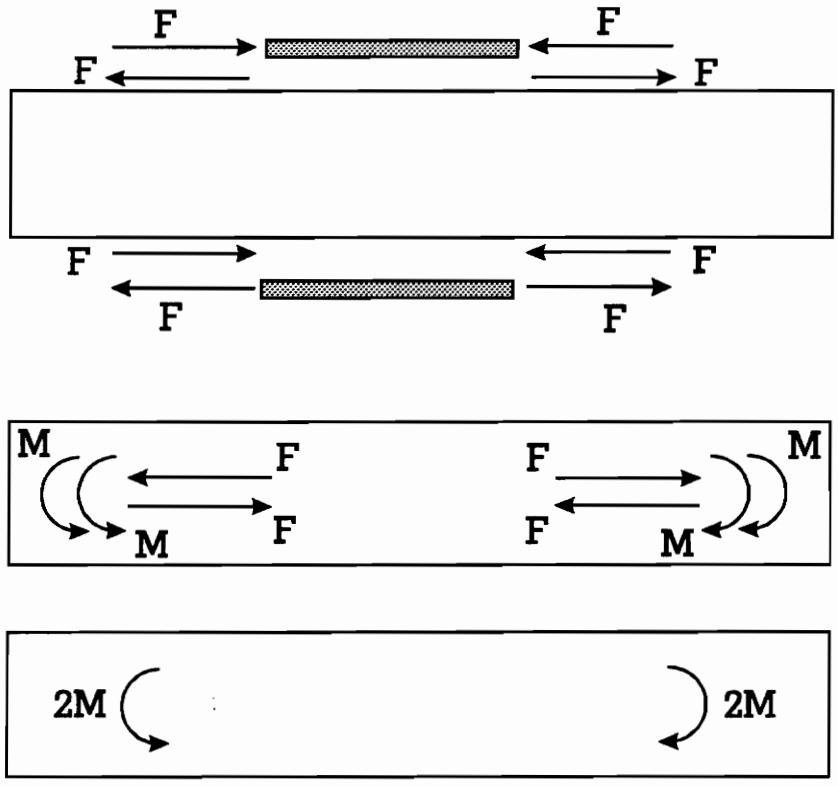

Figure 2.3. Bending Moment Produced by Two Piezoelectric Actuators

The strain throughout the beam that is caused by the bending moment will be assumed to be linear with the point of zero strain occurring at the neutral axis of the structure. According to Hooke's Law, the stress will be linear with zero stress occurring at the neutral axis (see Figure 2.4).

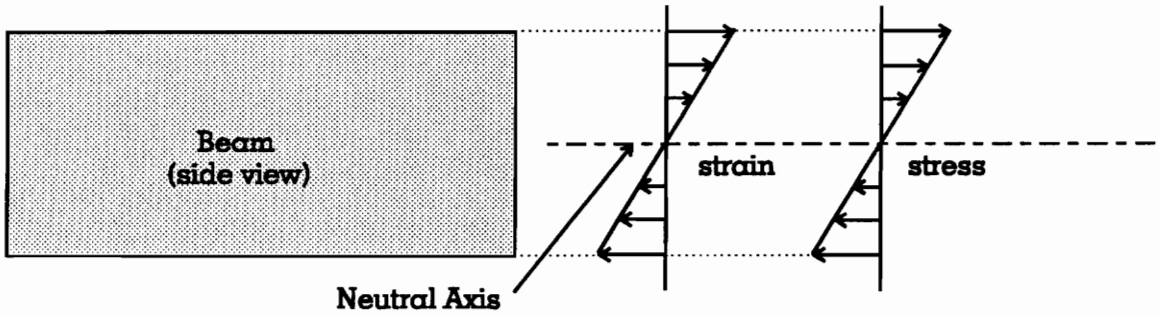

Figure 2.4. Strain and Stress Profile of the Structure

On the basis of the previous information, the equation for the bending moment acting on the beam can be derived. The equation for the bending moment, adapted from Crawley's work, that is acting through the structure normalized with respect to the width of the beam is

$$\frac{M_{tot}}{b} = \Lambda E_s t_s^2 \left(\frac{1}{3+\psi} \right) \tag{3}$$

where Mtot is the total moment acting at the neutral axis of the beam, b is the width of beam, and Λ is the induced strain of the piezoelectric actuator. The non-dimensional parameter, ψ, is identical to the previous case (see Eq. 2).

2.3 Axial Force and Bending Moment, One Piezoelectric Actuator

Figure 2.5 illustrates the free-body diagram of a beam and one piezoelectric actuator. Again, a perfect bonding layer is assumed to exist between the beam and the piezoelectric actuator. The induced strain of the piezoelectric actuator will result in a force acting at the pin connections. The resulting action on the beam is an axial force and a bending moment (see Figure 2.5). This differs from the cases where two piezoelectric actuators are used. Those cases involve either an axial force or a bending moment but not both.

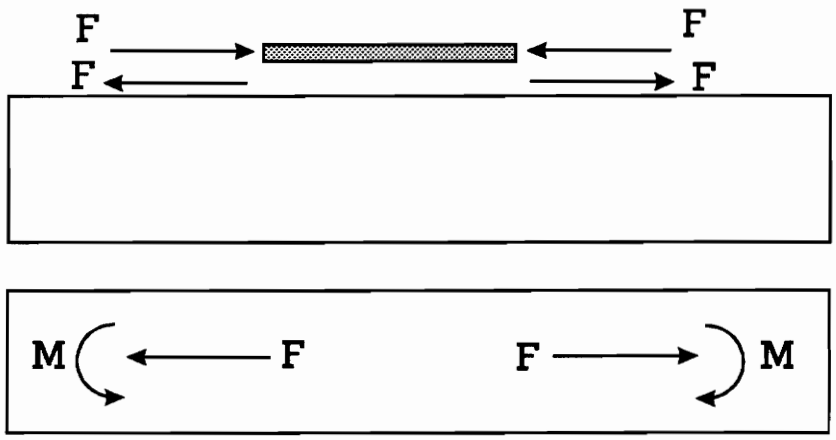

Figure 2.5. Axial Force and Bending Moment on the Host Structure

The equations for the axial force and bending moment, derived from Crawley's work, that are acting through the beam normalized with respect to its width are

$$\frac{F_{tot}}{b} = \Lambda E_s t_s \left(\frac{1}{1+\psi} \right)$$
$$\frac{M_{tot}}{b} = \frac{\Lambda E_s t_s^2}{2} \left(\frac{1}{3+\psi} \right) \tag{4}$$

Again, F_{tot} is the total force acting through the beam, M_{tot} is the total moment acting at the neutral axis of the beam, b is the width of beam, and Λ is the induced strain of the piezoelectric actuator. The values for the non-dimensional parameter, ψ, are identical to the two previous cases (see Equation 2).

2.4 Application of the Pin-Force Model to Several Layers

The previous applications of the pin-force model did not model a bonding layer between the piezoelectric actuator and the host structure. In addition to this, the stress throughout the host structure was linear and continuous. These assumptions allowed a simple derivation of the piezoelectric actuator system using the pin-force model. In actual systems, however, there is at least one layer, the bonding layer, between the piezoelectric actuator and the host structure. In this work, there are as many as three layers. It will be shown that members of several materials do not have a linear, continuous stress; therefore, a simple derivation of the piezoelectric actuator system cannot be performed using the pin-force model.

In order to use the pin-force model for several bonding layers, one approach is to transform the bonding layers and beam into one structure of like material that has a linear, continuous stress (Beer, 1981). This transformation is based on the assumption that the strain, ε_x, throughout each layer of the original structure is linear and continuous. In other words, plane sections remain plane before, during, and after bending. The equation for the linear, continuous strain is

$$\varepsilon_x = \frac{y}{\rho} \tag{5}$$

where y is the distance from the neutral axis to some point on the combined structure, and ρ is the radius of curvature of the combined structure under the action of pure bending. Figure 2.6 illustrates the stress and strain profiles of the untransformed structure considered in this work with the linear and continuous strain assumption.

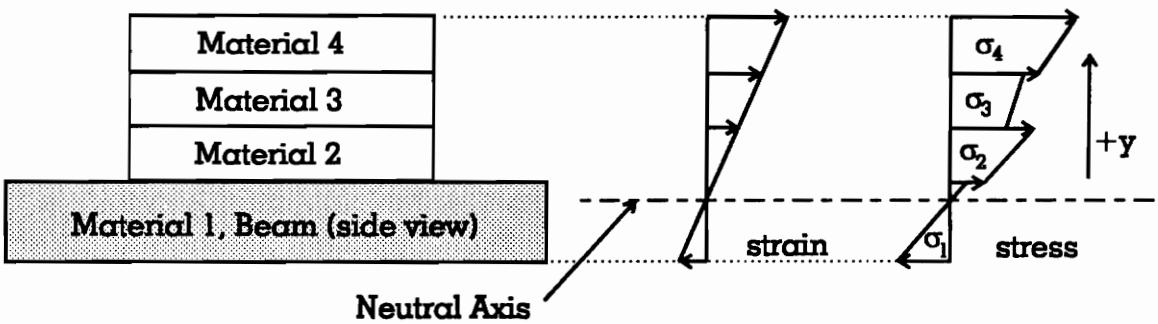

Figure 2.6. Multilayered Structure with a Linear, Continuous Strain Profile

Due to the different elastic moduli of the different materials, the stress throughout the entire thickness of the combined structure is not continuous. The stress, denoted by σ_i, in each portion of the structure can be equated as,

$$\sigma_i = E_i \varepsilon_x = \frac{E_i y}{\rho} \tag{6}$$

where E_i is the elastic modulus of the ith material.

Using the equations for stress in each material layer, the infinitesimal force acting on each material can also be obtained by

$$dF_i = \sigma_i dA_i = \frac{E_i y}{\rho} dA_i \tag{7}$$

The infinitesimal force through the ith layer is denoted by dF_i, and the infinitesimal area of the ith layer is denoted by dA_i. The infinitesimal area is calculated by

$$dA_i = m_i b dt \tag{8}$$

where b is the width of material one, m_i is the ratio of the width of the ith layer to the width of material one, and dt is an infinitesimal material thickness. If the width of each material is the same as material one, m_i will be unity. Figure 2.7 illustrates the geometry of the infinitesimal area.

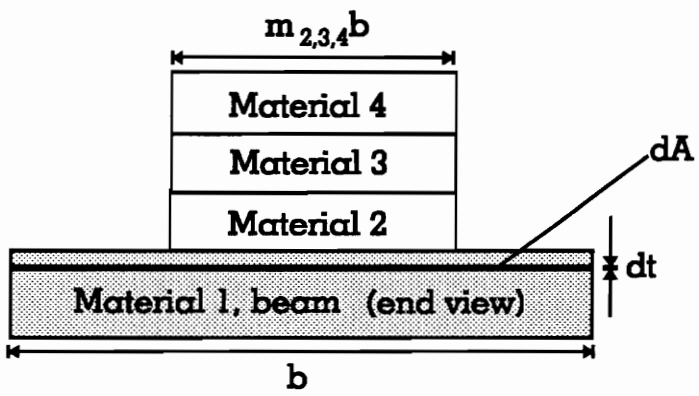

Figure 2.7. Geometry of the Infinitesimal Area, dA

The transformation of the bonding layers begins by assigning a constant, n_i, equal to the ratio of the elastic modulus of a bonding layer to the elastic modulus of the beam. The ratio is given by

$$n_i = \frac{E_i}{E_1} \tag{9}$$

where i is the material number. The constant, n_i, can be incorporated into the infinitesimal force equation to yield the following equation.

$$dF_i = \frac{E_i y}{\rho} dA_i = \frac{E_1 y}{\rho} m_i n_i dA_1 \tag{10}$$

The end result is a bonding layer with a transformed width of $m_i n_i b$ and elastic modulus of E_1. Figure 2.8 illustrates the geometry of the transformed structure, where $E_1 > E_2 > E_3 > E_4$.

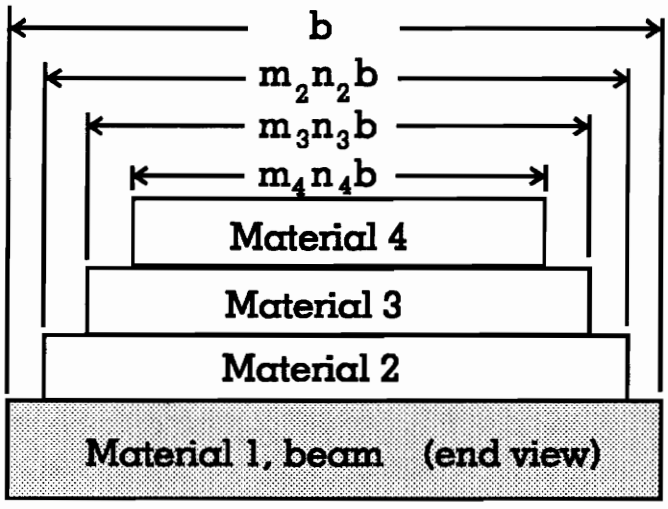

Figure 2.8. Geometry of the Transformed Structure

The stress throughout the transformed structure due to an axial force and bending moment will now be

$$\sigma_{ax} = \frac{F}{A_{tot}}$$
$$\sigma_b = \frac{My}{I} \tag{11}$$

The term σ_{ax} denotes the stress throughout the transformed structure due to an axial force, F, and σ_b denotes the stress throughout the transformed structure due to a bending moment, M. The term A_{tot} is the area of the transformed structure, y is the distance from the neutral axis of the transformed structure to some point on the structure, and I is the moment of inertia of the transformed structure.

The neutral axis of the transformed structure will be represented by $\overline{Y}$, which is the distance from the centroid of the cantilevered beam, material 1, to the neutral axis. The equation for $\overline{Y}$ is

$$\overline{Y} = \frac{\sum \overline{y}_i A_i}{\sum A_i} \tag{12}$$

where $\overline{y}_i$ is the distance from the centroid of the beam, material 1, to the centroid of the ith layer, and A_i is the area of the cross section of the ith layer. The direction for positive $\overline{Y}$ and $\overline{y}_i$ is the same for positive y (see Fig. 2.6). Simplifying this equation to involve a four layered structure yields

$$\overline{Y} = \frac{\left(\frac{t_1}{2}+\frac{t_2}{2}\right)(t_2 m_2 n_2)+\left(\frac{t_1}{2}+t_2+\frac{t_3}{2}\right)(t_3 m_3 n_3)+\left(\frac{t_1}{2}+t_2+t_3+\frac{t_4}{2}\right)(t_4 m_4 n_4)}{t_1 m_1 n_1 + t_2 m_2 n_2 + t_3 m_3 n_3 + t_4 m_4 n_4} \quad (13)$$

where t_i is the thickness of the ith structural layer. It should be noted that the thickness is not transformed; thus the thickness of a material is the same before and after transformation. The equation for the moment of inertia of the transformed structure is

$$I = \frac{1}{12} b \sum_{i=1}^{N} n_i m_i t_i^3 + b \sum_{i=1}^{N} n_i m_i t_i d_i^2 \quad (14)$$

where d_i is the distance from the centroid of the ith material layer to the neutral axis of the transformed structure, and N is the number of material layers in the structure; this work considers four layers. There is no sign convention for d_i since this value is squared. The equations for d_i of four material layers are stated as follows.

$$\begin{aligned} d_1 &= \overline{Y} \\ d_2 &= \frac{t_2}{2}+\frac{t_1}{2}-\overline{Y} \\ d_3 &= \frac{t_3}{2}+t_2+\frac{t_1}{2}-\overline{Y} \\ d_4 &= \frac{t_4}{2}+t_3+t_2+\frac{t_1}{2}-\overline{Y} \end{aligned} \quad (15)$$

The transformed structure has now been defined as a structure of one like material and linear, continuous stress. The equation for the stress in the transformed structure, Eq. 11,

can now be substituted in the pin-force model equation for one piezoelectric actuator to obtain the force and moment acting on the entire structure. The equations for the force, F, and the moment, M, acting on the combined structure normalized with respect to its untransformed width are as follows.

$$\frac{F}{b} = \Lambda\left[\frac{(E_1m_1t_1 + E_2m_2t_2 + E_3m_3t_3 + \cdots + E_im_it_i)(E_am_at_a)}{E_am_at_a + E_1m_1t_1 + E_2m_2t_2 + E_3m_3t_3 + \cdots + E_im_it_i}\right]$$

$$\frac{M}{b} = \Lambda\left[\frac{E_am_at_aE_1\frac{1}{b}I\left(\frac{t_1}{2} - \overline{Y} + t_2 + t_3 + \cdots + t_i\right)}{E_1\frac{1}{b}I + (E_am_at_a)\left(\frac{t_1}{2} - \overline{Y} + t_2 + t_3 + \cdots + t_i\right)^2}\right] \tag{16}$$

These equations hold for any number of layers. For a structure with four layers, the force and moment equations reduce to

$$\frac{F}{b} = \Lambda\left[\frac{(E_1m_1t_1 + E_2m_2t_2 + E_3m_3t_3 + E_4m_4t_4)(E_am_at_a)}{E_am_at_a + E_1m_1t_1 + E_2m_2t_2 + E_3m_3t_3 + E_4m_4t_4}\right]$$

$$\frac{M}{b} = \Lambda\left[\frac{E_am_at_aE_1\frac{1}{b}I\left(\frac{t_1}{2} - \overline{Y} + t_2 + t_3 + t_4\right)}{E_1\frac{1}{b}I + (E_am_at_a)\left(\frac{t_1}{2} - \overline{Y} + t_2 + t_3 + t_4\right)^2}\right] \tag{17}$$

The equation for the bending moment and axial force produced by one piezoelectric actuator with three bonding layers has been derived. These equations will serve as a theoretical predictor of the authority of the actual system.

CHAPTER 3
DYNAMIC RESPONSE CHARACTERISTICS

We expect each attachment technique will affect the dynamic response characteristics of the beam. The frequency response functions, authority levels, and damping ratios for each attachment technique are the dynamic response characteristics that will be considered for observation in this work. In this chapter, we will describe how each of these characteristics is quantified.

3.1 Statistical Analysis

The purpose for conducting a statistical analysis is to quantify the individual effects of several different samples into one interval of values, the confidence interval. The confidence interval indicates the repeatability of the measured data, thereby revealing how well each sample represents the entire population. For the attachment technique involving a piezoelectric actuator attached to the beam with wax, five samples were used in the statistical analysis. Ten samples were used for the other attachment techniques. The following values for each attachment technique will be calculated as a part of the statistical analysis:

- sample mean of the frequency response function magnitude, phase angle, and coherence
- sample standard deviation of the frequency response function magnitude, phase angle, and coherence

- 95% confidence interval of the frequency response function magnitude, phase angle, and coherence
- coefficients of the linear least squares approximation for the change in authority
- coefficients of the linear least squares approximation for the change in the damping ratio of the third mode of vibration

The sample mean, $\overline{x}$, of the frequency response functions will be calculated at each frequency point. The sample mean will be used to calculate the sample standard deviation, s_x, at each frequency point. The sample mean and sample standard deviation provide unbiased estimates of the population mean and population standard deviation (Bendat, 1986). From this information, the confidence intervals will be calculated for the population mean, μ_x. In order to do this, a normal distribution of the sample data must be assumed (Beckwith, 1993). The following equations will be used for the calculations at each frequency point

$$\overline{x} = \frac{1}{N}\sum_{i=1}^{N} x_i \tag{1}$$

$$s_x^{\,2} = \frac{1}{N-1}\sum_{i=1}^{N}\left(x_i - \overline{x}\right)^2 \tag{2}$$

$$\overline{x} - \frac{s_x t_{\alpha/2}}{\sqrt{N}} \le \mu_x < \overline{x} + \frac{s_x t_{\alpha/2}}{\sqrt{N}} \tag{3}$$

where x_i is the sample data value, N is the number of samples, and $t_{\alpha/2}$ is the t-distribution value. The t-distribution value is used to calculate confidence intervals when the number of samples is less than 30 (Beckwith, p.70).

Another statistical procedure will be used to determine the change in actuator authority and change in damping ratio as a function of removals from the host structure. The authority of the actuator will be represented by the magnitude of the frequency response function. The magnitude will not be considered at each frequency point but only at the principal modes. To calculate the change in authority and change in damping ratio, each value will be paired with the number of times the actuator has been removed from the host structure. The removals are numbered 0 through 9, and an arbitrary linear relationship for the change in authority and change in damping ratio as a function of the number of removals is assumed. The following equation describes this relationship (Walpole, 1993),

$$\hat{u} = c_0 + c_1 x \tag{4}$$

where the term $\hat{u}$ is the estimated value of the authority or the damping ratio, c_0 is the intercept of the linear change in magnitude, c_1 is the slope of the linear change in magnitude, and x is the removal number. The linear regression coefficients, c_0 and c_1, will be calculated using the following matrix equation

$$C = (X'X)^{-1} X'U \tag{5}$$

where C is a matrix containing the values of c_0 and c_1, U is a column matrix that contains the experimental frequency response function magnitude or damping ratio, and X is a matrix containing ones in the first column and the removal number in the second column (Walpole, 1993). This method of obtaining the linear regression coefficients was chosen in order to utilize matrix math operations to obtain the solution.

3.2 Quantifying the Authority Levels of Each Attachment Technique

The authority levels of the piezoelectric actuator are expected to be different for each attachment technique. In order to determine the differences, the authority levels of each attachment technique will be observed in two ways. One is to observe the differences in authority due to the different bonding layers of each attachment technique. The second way is to observe the differences in authority due to removing the actuator from the beam. Experimental values of actuator authority and authority reduction will be obtained. A theoretical calculation of the actuator authority of each attachment technique will be made in order to verify the analytical model of the piezoelectric actuator and bonding layers.

3.2.1 Differences in Authority due to Different Attachment Techniques

Each attachment technique involves bonding layers of different physical parameters. These different physical parameters will affect the authority of each actuator on the beam. The sample mean of the magnitude of the frequency response function will be used to describe the authority obtained from experimental tests. Only the first application of the removable, reusable actuator will be considered. The theoretical value of the bending moment applied to the beam will also be used to describe the differences in authority caused by the different physical parameters of each attachment technique. The theoretical values will be compared to the experimental values in order to determine the validity of the analytical model.

On the basis of the analytical model described in Chapter 2, the potential effects of the different physical parameters are that the farther the actuator is from the neutral axis of the beam, the greater the bending moment. In addition to this, the stiffer the elastic modulus of the bonding layer, the smaller the bending moment that will be transmitted to the beam. In other words, for a given thickness, the stiffer attachment technique will produce a smaller authority. Likewise, for a given stiffness, the thicker attachment technique will produce a greater authority. These differences can be observed from the numerical values of the authority level for each attachment technique contained in Chapter 5.

3.2.2 Differences in Authority due to Removing the Actuator

As was previously stated, the removable, reusable piezoelectric actuators will be removed from the host structure so that they can be reused several times. Removing the actuator from the host structure will involve some deformation of the actuator. The deformation will be dependent upon the strength of the material that bonds the actuator to the host structure. In other words, a strong bond will require more deformation to break the bond. By measuring the authority of each attachment technique after each removal from the beam, the change in authority will be observed. The attachment technique that involves the most significant deformation to the piezoelectric actuator during removal of the actuator system is presumed to exhibit the most significant loss in actuation authority.

The sample mean of the magnitude of the frequency response function will be used to experimentally determine the change in actuation authority for each attachment technique. The change in authority will only be observed at the principal modes. By observing the

magnitude as a function of removals from the structure, the slope of a linear, curve fitted line will reveal the change in authority.

3.3 Quantifying the Damping Ratios of Each Attachment Technique

We expect the damping ratios of each attachment technique to be different from each other for two reasons. First of all, we expect the damping ratios to be different because the bonding layers of each attachment technique are different. Secondly, we expect the damping ratios to be different because the deformations to the piezoelectric actuator of each attachment technique during removal are different. This section will discuss these differences in more detail as well as explain how the damping ratios will be quantified.

3.3.1 Differences in Damping Ratios due to Different Attachment Techniques

Constructing a removable, reusable actuator involves adding to the permanent attachment technique different, and in some cases extra, bonding layers to the piezoelectric actuator. These different bonding layers will change the physical parameters of the system, thus potentially changing the damping ratio values. For a single degree of freedom system with viscous damping, changes in the damping ratio will affect the magnitude and phase angle of its frequency response function. The following equations verify this statement (Thompson, 1993).

$$\frac{Xk}{F_0} = \frac{1}{\sqrt{\left[1-\left(\frac{\omega}{\omega_n}\right)^2\right]^2 + \left[2\zeta\left(\frac{\omega}{\omega_n}\right)\right]^2}} \tag{7}$$

$$\tan\phi = \frac{2\zeta\left(\frac{\omega}{\omega_n}\right)}{1-\left(\frac{\omega}{\omega_n}\right)^2} \tag{8}$$

$\frac{Xk}{F_0}$ is the non dimensional magnitude of the frequency response function, ϕ is the phase angle of the frequency response function, ω is the excitation frequency, ω_n is the natural frequency of the system, k is the spring constant of the single degree of freedom system, and ζ is the damping ratio.

On the basis of the previous equations, the damping ratios for the piezoelectric actuators of each attachment technique will be calculated using a single degree of freedom curve fit. To narrow the scope of this observation, the curve fit will involve only one structural mode. The third structural mode will be used because it has few closely spaced modes in its frequency vicinity and the confidence intervals in this frequency region are typically smaller than other modes (see Chapter Five).

3.3.2 Differences in Damping Ratios due to the Removing the Actuator

The removal process involves some deformation to the piezoelectric actuator, and the deformation for each attachment technique is different. The attachment technique that cemented the piezoelectric actuator to an aluminum stiffener and then cemented the stiffener to the structure involved large deformation to the piezoelectric actuator during removal. The other attachment techniques, involving wax, experienced insignificant deformation.

The damping ratios of each attachment technique will be calculated at the third structural mode. They will be calculated for each removal of the actuator. This information will be used to calculate the coefficients of a linear, least squares approximation of the change in damping as a function of removals from the beam. The coefficients will quantify the change in damping ratios for each attachment technique.

The dynamic response characteristics of the beam have been outlined with regard to each attachment technique. Methods of quantifying these characteristics have also been included. These characteristics form the basis of the experiments for this work, and the next chapter outlines the experiment design.

CHAPTER 4
EXPERIMENT DESIGN

The experiments that were performed involved a number of test articles and measuring devices. This chapter is devoted to describing these items in detail. The experimental procedures will also be outlined. Preceding this information will be the experimental approach, which describes how the experimental data will be used in this research.

4.1 Experimental Approach

The approach used to characterize the influence of a removable and reusable piezoelectric actuator on a cantilevered beam was to perform a set of experiments that would measure the frequency response function and coherence function between the removable, reusable piezoelectric actuator and the beam. The frequency response function and coherence function were measured for ten applications of the actuator system. The frequency response function was a ratio of the tip acceleration the beam to the input voltage of the piezoelectric actuator. In order to establish a sample population that could be used to form statistical information about the total population of all actuators, several samples of each attachment technique were used in the experiments. Five samples were used for the attachment technique that involved a piezoelectric actuator attached to the structure with wax. Ten samples were used for the other attachment techniques. The frequency response function and coherence function for a similar cantilevered beam excited by an electromagnetic shaker were also measured for comparison.

4.2 Experiment Setup

The host structure that was tested was a 34.3 cm x 3.8 cm x 0.32 cm cantilevered aluminum beam. Four different actuator attachment techniques were used. The piezoelectric element in each actuator was the same, but the bonding layers of the piezoelectric actuator were different for each attachment technique. The piezoelectric element was a 3.2 cm x 1.9 cm x 0.0191 cm Piezoelectric Products, Inc. piezoelectric actuator, type G1195. For the permanent attachment technique, the piezoelectric actuator was cemented to the beam with strain gauge cement. The strain gauge cement that was used was M-Bond 200 Adhesive by Measurements Group, Inc. The next attachment technique involved a piezoelectric actuator cemented to an aluminum stiffener and the stiffener cemented to the beam. The cement that was used was M-Bond 200, and the aluminum stiffener had dimensions of 3.33 cm x 2.06 cm x 0.0794 cm, which are slightly larger than those of the piezoelectric element. The next attachment technique involved cementing the piezoelectric actuator to an aluminum stiffener with M-Bond and then attaching the stiffener to the beam with wax made by Kistler Instrument Corporation, part number 8432. The stiffener in this actuator is identical to the one previously described. The last attachment technique attached the piezoelectric actuator to the beam using only wax. Each actuator system was centered on the width of the beam, 1.27 cm from the base.

The input voltage to the actuator was reduced for measurement using a voltage divider since the input voltage alone was too large for the analyzer to accommodate. The acceleration of the beam tip was measured using a Kistler model 8622 accelerometer that was attached with a threaded stud, centered at 0.318 cm from the end of the beam. For

the case of the piezoelectric actuator attached to the beam with wax, a similar accelerometer without the threaded stud was used. This accelerometer was attached to the beam with wax in order to electrically insulate the accelerometer from the piezoelectric actuator. The signal from both accelerometers was conditioned by a Kistler model 5122 Piezotron Coupler. A Tektronix model 2630 Fourier Analyzer was used to acquire and record the time data from the actuator and accelerometer as well as supply the input signal to the actuator. The measurements were obtained using AC coupling. For the Tektronix analyzer, AC coupling removes all frequencies below 3 Hz. The input signal was amplified using a Realistic MPA-25, 20 Watt P.A. power amplifier and further amplified with a 50:1 voltage gain transformer. The Realistic amplifier has a frequency attenuation between 0 an 100 Hz, and below 20 Hz, the amplifier is not effective. Therefore, the lower bound on usable data is 100 Hz.

The shaker tests were conducted using a Ling Dynamic Systems Ltd. Model 200 Series electromagnetic shaker. A Kistler model 9712A50 force transducer measured the force being transferred to the cantilever beam. This signal was conditioned using the same signal conditioner used for the accelerometer in the piezoelectric actuator tests. The force was centered on the width of the beam and applied 2.86 cm from the base. The tip acceleration was measured and conditioned with the same accelerometer and conditioner that were used for the piezoelectric actuator tests, and the time data from the force transducer and accelerometer were acquired with the Tektronix Fourier Analyzer.

Figures 4.1 and 4.2 illustrate the experimental setups for the piezoelectric actuator and shaker tests, respectively. These figures are located at the end of the chapter.

4.3 Experiment Procedure

Using the experimental setup, the actuators were excited with burst random signals over a 2 kHz range. Using the Tektronix Fourier Analyzer, ten samples were measured and averaged to obtain one frequency response function and one coherence function. The removable actuators were removed and reapplied, and the test was performed again. The application process was performed ten times except for the permanently attached piezoelectric actuator; it was applied only once. The frequency response function using the electromagnetic shaker was performed with burst random signals over a 2 kHz range. The frequency response function and coherence function were measured using similar techniques.

4.4 Post Data Processing

The data obtained from the Tektronix Fourier Analyzer was subsequently processed using Matlab (Math Works, 1993). The post data processing was performed in order to obtain the statistical information about each attachment technique. In addition to this, Modhan (Han, 1990), a curve fitting, computer algorithm, was used to perform the curve fits that would yield the damping ratio values.

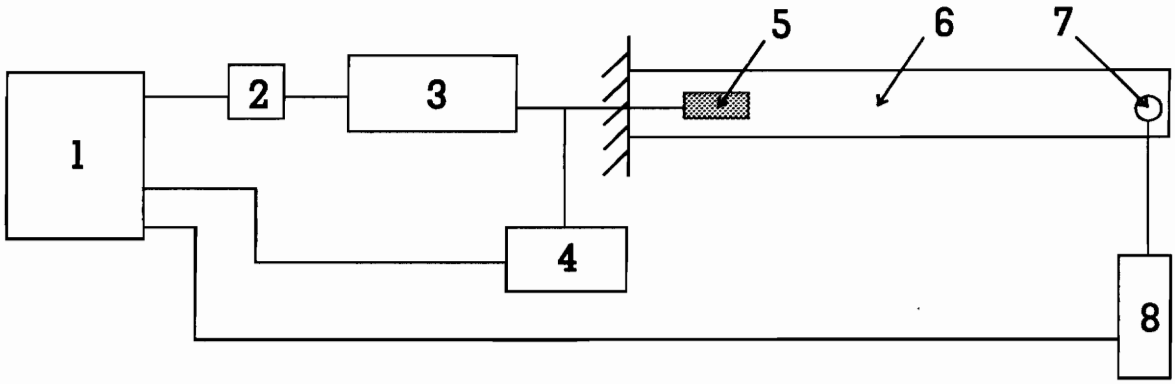

1 FFT Analyzer
2 Transformer
3 Amplifier
4 Voltage Divider
5 Piezoelectric Actuator
6 Cantilevered Beam
7 Accelerometer
8 Signal Conditioner

Figure 4.1. Experimental Setup for the Piezoelectric Actuator Tests

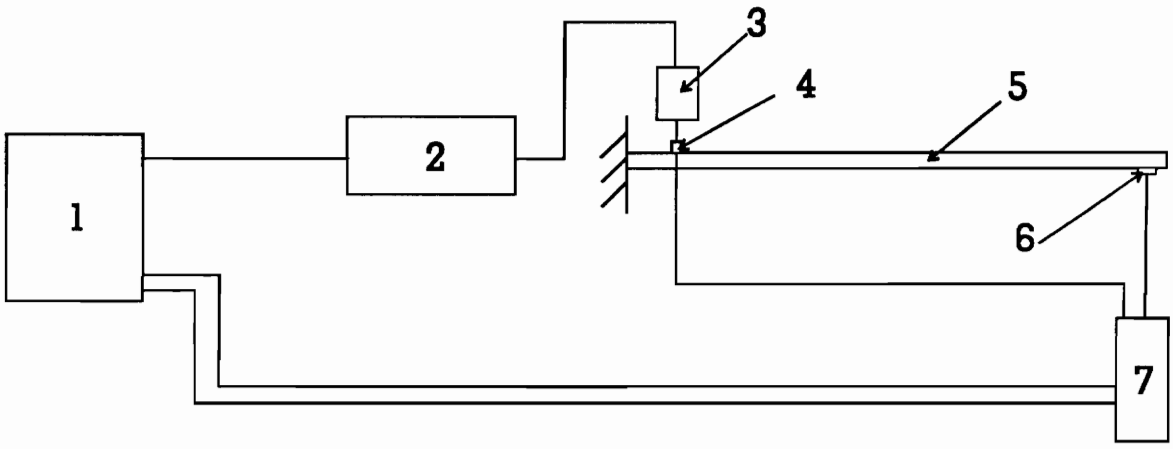

1 FFT Analyzer
2 Amplifier
3 Shaker
4 Force Transducer
5 Cantilevered Beam
6 Accelerometer
7 Signal conditioner

Figure 4.2. Experimental Setup for the Shaker Tests

CHAPTER 5
RESULTS AND OBSERVATIONS

The results of the experiments and analyses are presented in this chapter. First, the frequency response functions of each attachment technique will be presented and analyzed. A presentation and analysis of the authority levels of each attachment technique will then follow. Next, the damping ratios of each attachment technique will be presented and analyzed. A qualitative analysis of the ease of use of each attachment technique will be presented. A comparison of the response of the cantilevered beam excited by an electromagnetic shaker will be compared to the response from a piezoelectric actuator. Observations about the coherence of the frequency response function will also be made. Finally, the location of an antiresonance around the fourth mode of vibration will be discussed.

5.1 Statistical Analysis of Confidence Intervals

The confidence intervals of the mean magnitude, phase angle, and coherence of the frequency response functions were calculated. The confidence intervals correspond to the first application of each attachment technique. Figures 5.1.1 through 5.1.4 illustrate the results. Appendix A contains plots of selected, individual samples that were used to form the confidence intervals.

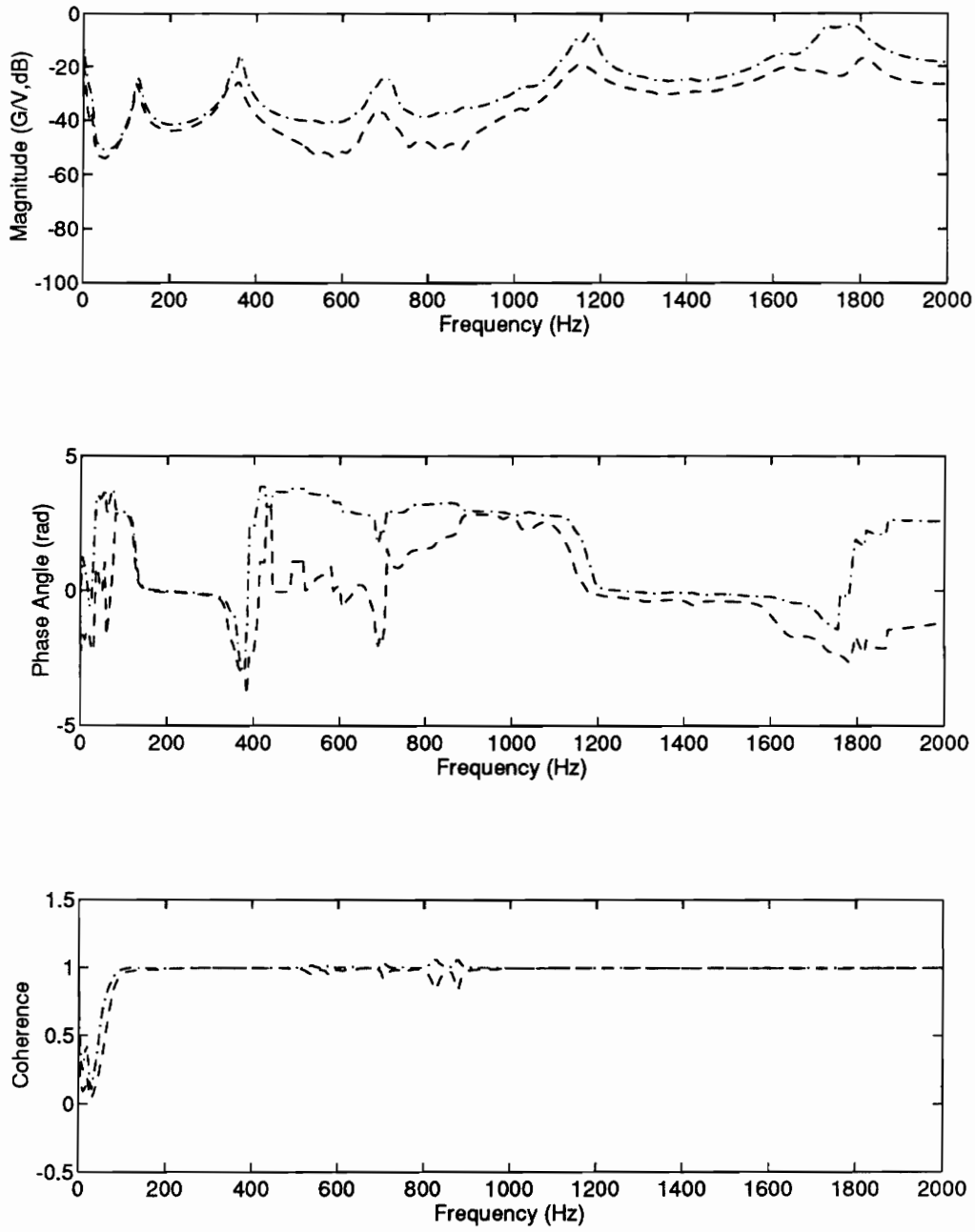

Figure 5.1.1. Confidence Intervals of the Mean Magnitude, Phase Angle, and Coherence of the Frequency Response Function for the Piezoelectric Actuator, Cement, Beam, Attachment Technique

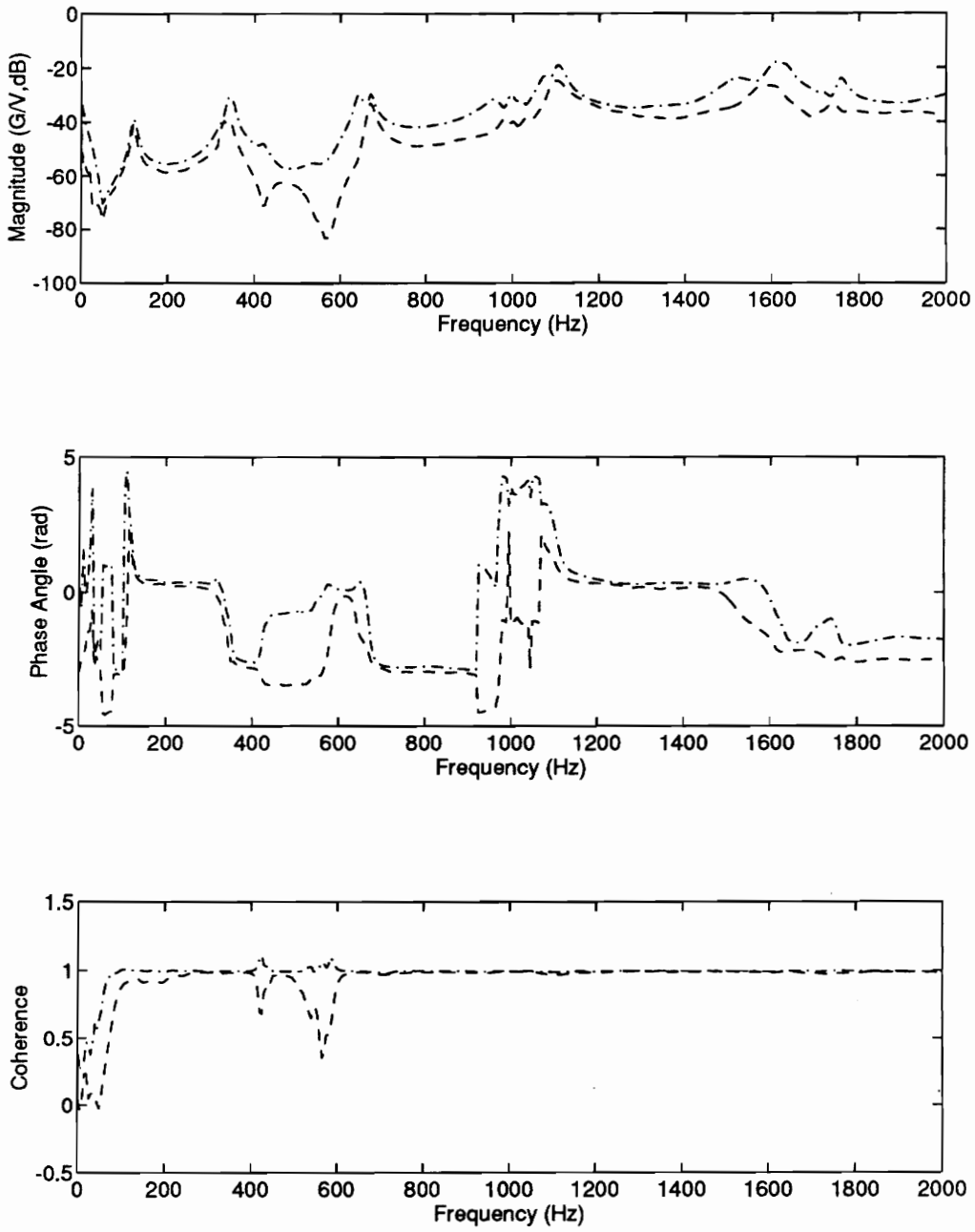

Figure 5.1.2. Confidence Intervals of the Mean Magnitude, Phase Angle, and Coherence of the Frequency Response Function for the Piezoelectric Actuator, Wax, Beam, Attachment Technique

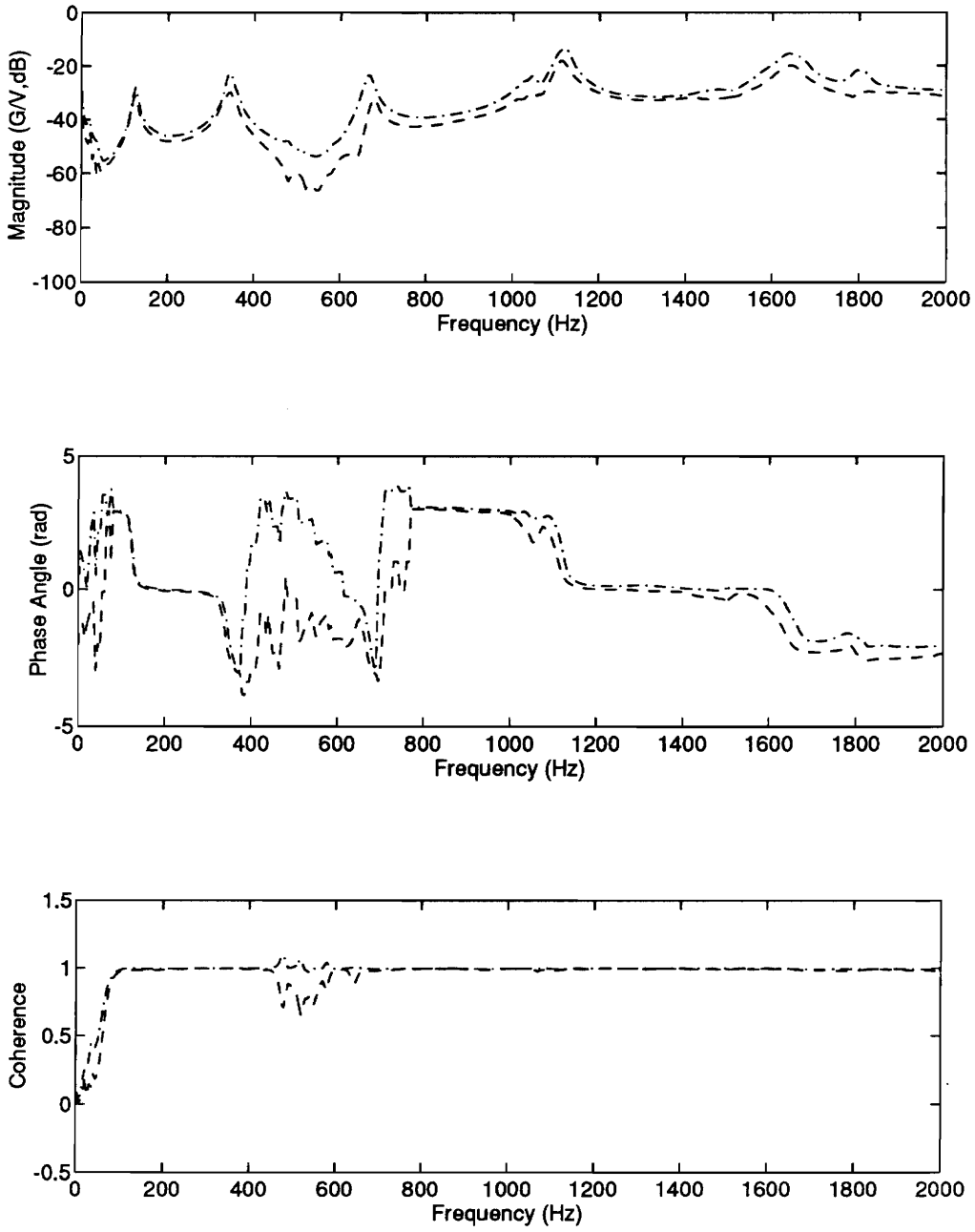

Figure 5.1.3. Confidence Intervals of the Mean Magnitude, Phase Angle, and Coherence of the Frequency Response Function for the Piezoelectric Actuator, Cement, Stiffener, Cement, Beam, Attachment Technique

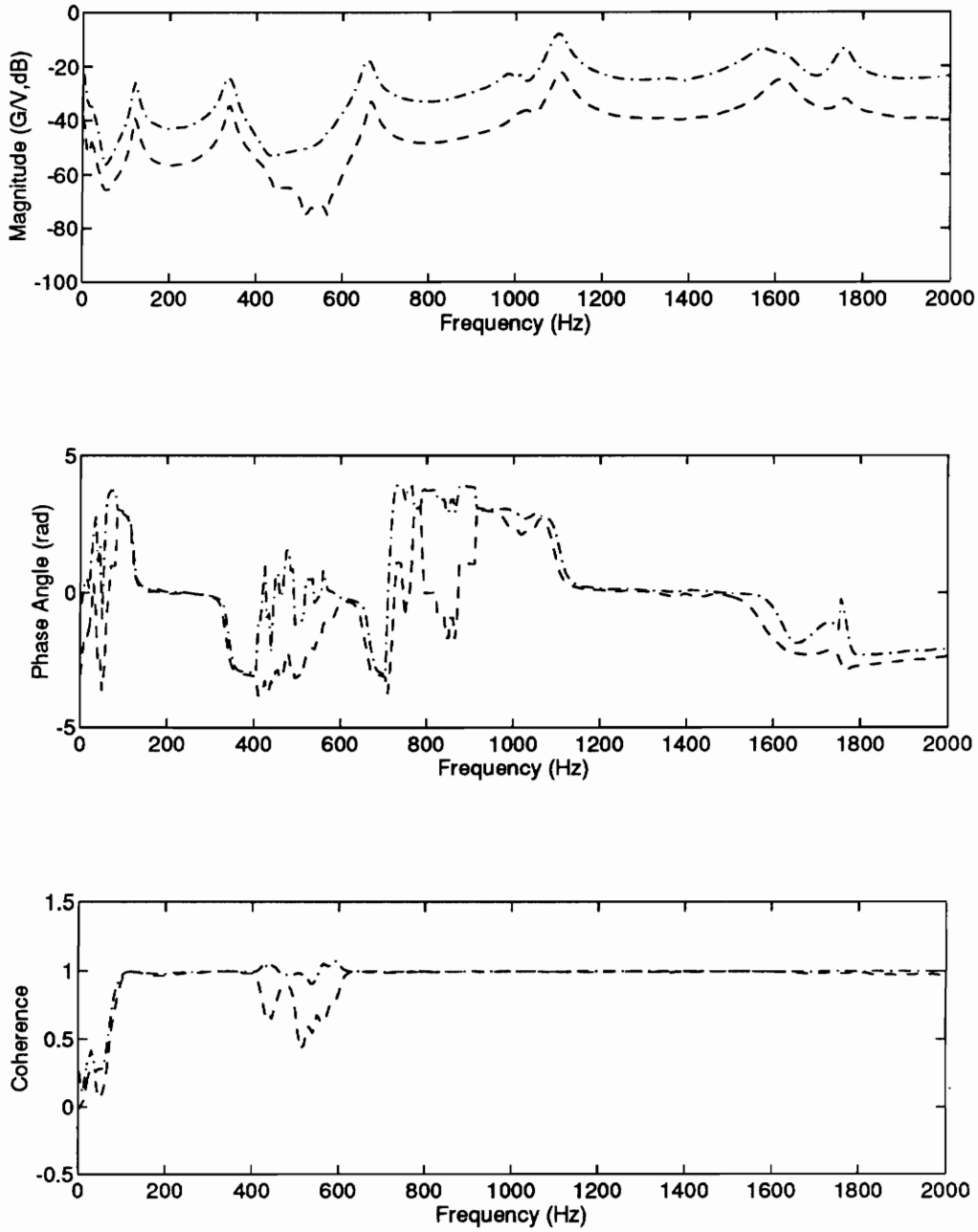

Figure 5.1.4. Confidence Intervals of the Mean Magnitude, Phase Angle, and Coherence of the Frequency Response Function for the Piezoelectric Actuator, Cement, Stiffener, Wax, Beam, Attachment Technique

The confidence intervals of the mean magnitude and phase angle of the frequency response functions were largest in two main areas, areas of antiresonance and areas of closely spaced modes. For the permanent attachment technique, an antiresonance occurred either between 400 to 600 Hz or between 700 to 900 Hz. For the other attachment techniques, an antiresonance occurred only in the frequency region from 400 to 600 Hz. The previous figures illustrate the large confidence intervals in these regions. Large confidence intervals also occurred at frequencies above 1500 Hz. These frequencies contain several closely spaced modes. The attachment technique that involved a piezoelectric actuator attached to the structure with wax also contained closely spaced modes between 900 and 1100 Hz (see Figure 5.1.2). Large confidence intervals for the mean magnitude and phase angle also occurred in this region. The large confidence intervals described in this paragraph signify that the frequency of the antiresonance varied from one sample to another. The large confidence intervals also signify that the frequency and presence of closely spaced modes varied from one sample to another.

The confidence intervals for the mean magnitude and phase angle were generally smallest in the frequency region from 100 to 400 Hz. The samples in these regions had no antiresonances and exhibited widely spaced modes.

The confidence intervals of the mean coherence were largest in the areas containing antiresonance, from 400 to 600 Hz. The coherence of the frequency response function is low in the areas of antiresonance because the response of the system is close in magnitude to the noise floor of the measuring devices. The resulting output signal is uncorrelated with the input, thereby creating a low coherence value in that frequency range. Unlike the confidence intervals for the mean magnitude and phase angle, the confidence intervals of

the mean coherence were small and close to unity in frequency regions containing closely spaced modes. This signified good correlation between input voltage and tip acceleration in these regions.

5.2 Authority Levels

The authority levels for each attachment technique were calculated and evaluated. Both experimental and theoretical observations were made with regard to which attachment technique provided the greatest actuation authority. The change in authority over several removals of the actuator was also calculated for each attachment technique from the experimental data.

5.2.1 Differences in Authority due to Different Attachment Techniques

The theoretical values for force and bending moment of each attachment technique are located in Table 5.2.1. These values were calculated using the physical parameters in Table 5.2.2 along with a unit micro strain as the induced strain of the piezoelectric actuator. Table 5.2.2 contains estimations for the elastic modulus of the cement and wax. These estimates were made because no information from the manufacturer was available for these parameters. Only the bending moment will be considered when describing the authority level of each attachment technique since the extension force does not contribute to the lateral vibration of the tip of the structure.

Table 5.2.1. Numerical Values for Extension Force and Bending Moment Through the Structure

Attachment Technique	Extension Force, N	Bending Moment, N-m
piezoelectric actuator, cement, beam	2.88	0.0093
piezoelectric actuator, wax, beam	2.89	0.0095
piezoelectric actuator, cement, stiffener, cement, beam	2.56	0.0124
piezoelectric actuator, cement, stiffener, wax, beam	2.55	0.0126

Table 5.2.2. Physical Parameters of the Actuators, * denotes an estimation

Material	Elastic Modulus, GPa	Thickness, μm
Cantilevered Beam	71.0	3175
Stiffener	71.0	793.8
Cement between piezoelectric actuator and beam	53.3*	114.3
Wax between piezoelectric actuator and beam	35.5*	165.1
Cement between piezoelectric actuator and stiffener	53.3*	38.10
Wax between piezoelectric actuator and stiffener	35.5*	88.90
Piezoelectric Actuator	63.0	190.5

For the theoretical calculations, the attachment technique that provided the greatest bending moment was the one that attached the piezoelectric actuator to a stiffener with cement and the stiffener to the structure with wax. The attachment technique that attached the piezoelectric actuator to the stiffener with cement and the stiffener to the structure with cement provided the next greatest bending moment. The next greatest bending moment was provided by the piezoelectric actuator that was attached to the

structure with wax, and the smallest bending moment was provided by the piezoelectric actuator that was attached to the structure with cement. In short, the piezoelectric actuators that were separated from the structure with the greatest distance provided greater bending moments than the ones that were closer. Also, the piezoelectric actuators that incorporated wax into their attachment technique provided greater bending moments than similar attachment techniques that used cement.

The authority levels observed in the experimental data were referred to in terms of the magnitude of the frequency response function at each mode. The values and their 95% confidence intervals are stated in Table 5.2.3, and Figs. 5.2.1 through 5.2.4 illustrate the magnitude of the frequency response function. When comparing the authority level of one attachment technique to another, the order of increasing authority was different at different modes. In other words, some attachment techniques exhibited the greatest actuation authority over other actuators at some modes but not at others.

Table 5.2.3. Actuation Authority Level for Each Mode of Vibration (G's/volt, dB)

Bonding Technique	mode 2	mode 3	mode 4	mode 5	mode 6
piezoelectric actuator, cement, beam	-25.4 ± 1.3	-20.9 ± 4.9	-30.7 ± 6.1	-14.0 ± 6.4	-11.6 ± 6.2
piezoelectric actuator, cement, stiffener, cement, beam	-29.4 ± 1.5	-26.3 ± 3.5	-29.2 ± 5.4	-16.0 ± 2.2	-17.6 ± 2.2
piezoelectric actuator, cement, stiffener, wax, beam	-32.7 ± 6.6	-29.6 ± 5.0	-25.8 ± 7.3	-15.3 ± 7.3	-20.1 ± 4.8
piezoelectric actuator, wax, beam	-40.0 ± 0.9	-35.3 ± 4.6	-31.3 ± 1.7	-21.8 ± 2.9	-22.3 ± 4.4

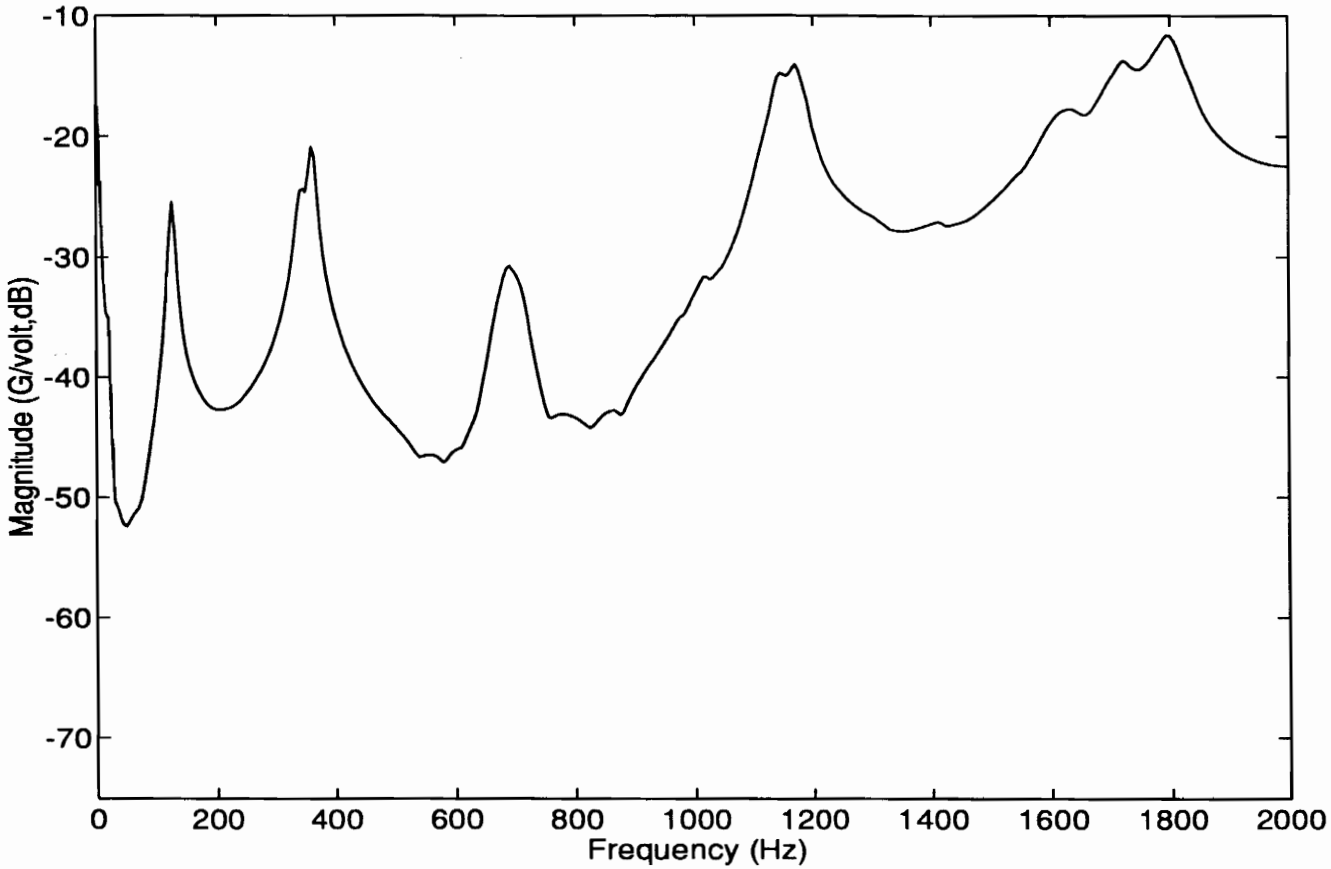

Figure 5.2.1. Sample Mean of the Frequency Response Function Magnitude for the Piezoelectric Actuator, Cement, Beam Attachment Technique

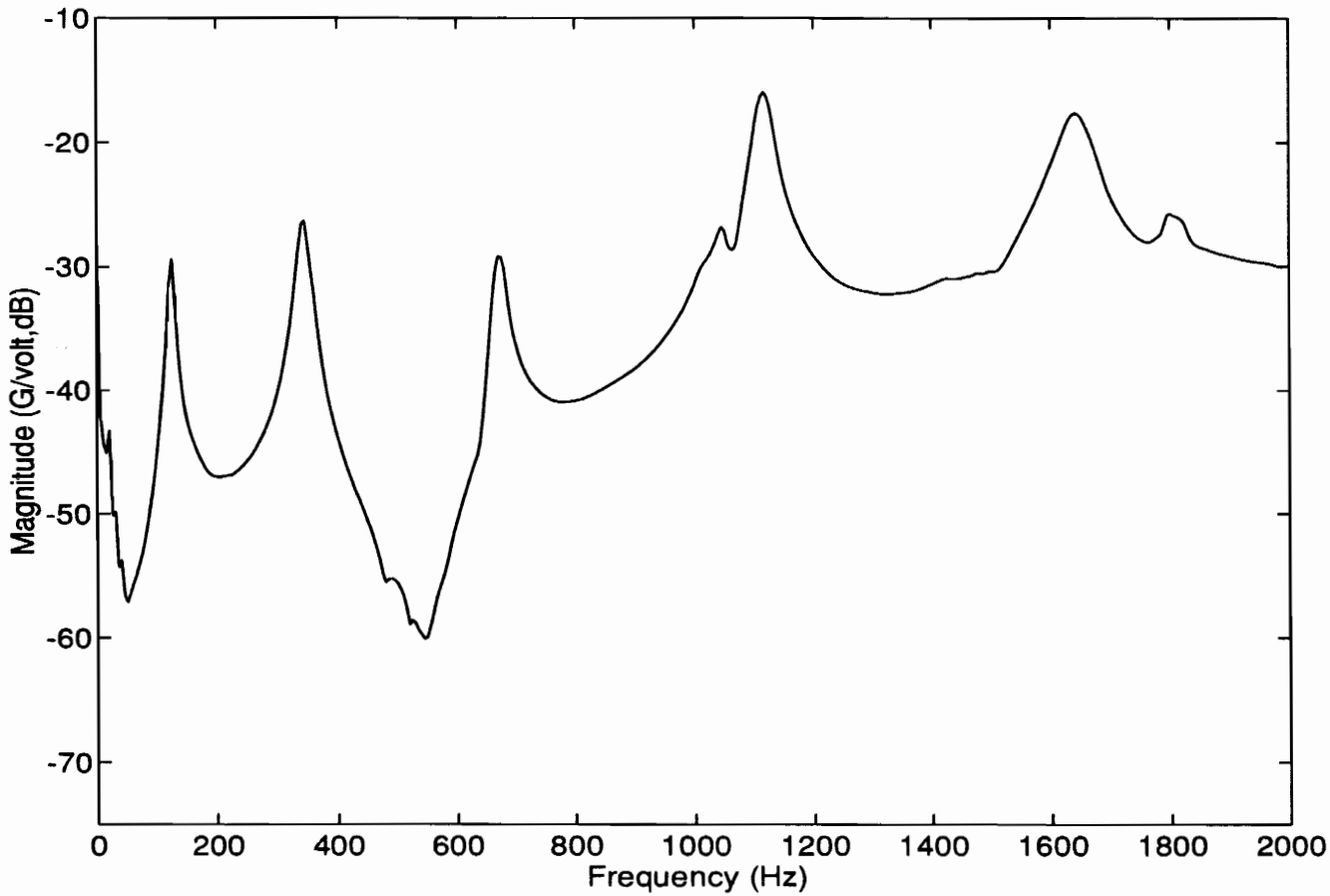

Figure 5.2.2. Sample Mean of the Frequency Response Function Magnitude for the Piezoelectric Actuator, Cement, Stiffener, Cement, Beam Attachment Technique

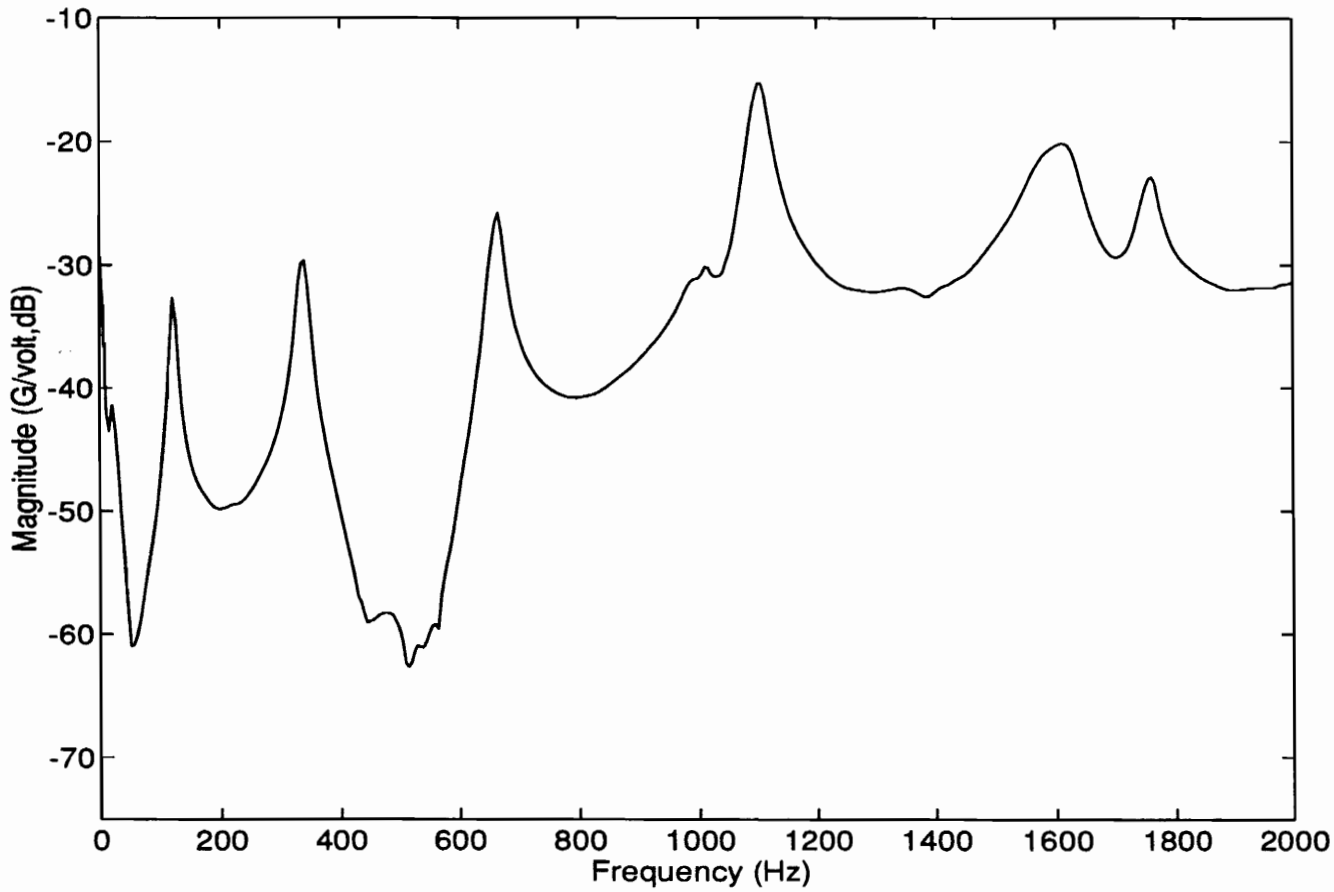

Figure 5.2.3. Sample Mean of the Frequency Response Function Magnitude for the Piezoelectric Actuator, Cement, Stiffener, Wax, Beam Attachment Technique

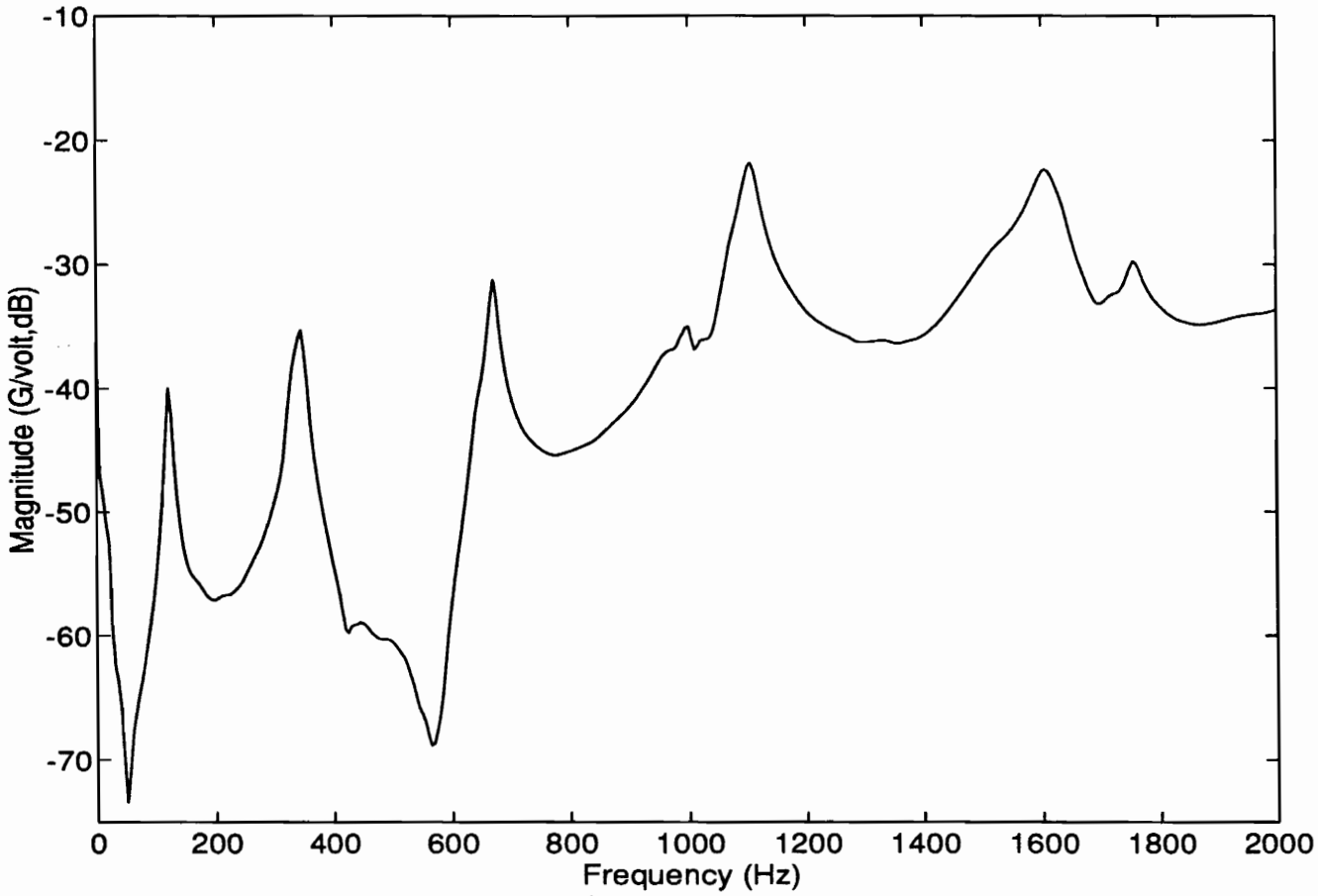

Figure 5.2.4. Sample Mean of the Frequency Response Function Magnitude for the Piezoelectric Actuator, Wax, Beam Attachment Technique

The attachment technique that involved a piezoelectric actuator cemented to the structure had the highest authority over the other attachment techniques except at the fourth mode. At the fourth mode, the attachment technique that involved a piezoelectric actuator cemented to a stiffener and the stiffener attached to the structure with wax had the highest authority.

The authority levels observed in the experimental data were different from the authority levels predicted from the pin-force model. The theoretical calculations from the pin-force model revealed that attachment techniques where piezoelectric actuators were far from the surface of the beam had higher authority levels than those where the piezoelectric actuators were close to the beam's surface. The experimental results revealed that the highest authority, with the exception of the fourth mode, belonged to the attachment technique involving the piezoelectric actuator that was closest to the beam.

The theoretical calculations also revealed that attachment techniques involving wax yielded authorities greater than those involving cement. The experimental values revealed that for most modes of vibration, attachment techniques involving wax had smaller authorities than those involving cement. In particular, the attachment technique involving a piezoelectric actuator cemented to a beam had higher authority levels at all modes over the attachment technique that involved a piezoelectric actuator attached to the beam with wax.

The methods for transforming beams of several materials into an equivalent beam of one material are common to most texts on structural mechanics (Beer, 1981; Shames, 1975;

Levinson, 1971). These methods were incorporated into the pin-force model in order to calculate the bending moment in a cantilevered beam. The primary assumption in these methods is that plane sections remain plane. This assumption can be proven for symmetric beams of one material (Beer, 1981; Shames, 1975), but no proof of this assumption was made for beams of several materials.

As the elastic modulus of each layer of a multilayered beam approaches one common elastic modulus, the multilayered beam becomes a beam of homogeneous material. It was previously stated that for symmetric beams of one material, the assumption that plane sections remain plane can be proved. It can be inferred that the closer the elastic modulus of each material is to one common elastic modulus, the closer that the assumption that plane sections remain plane will be true. In other words, this assumption is not accurate for materials with significantly different elastic moduli, and the methods of calculating the bending moment from the pin-force model are no longer accurate.

The elastic modulus for the cement and wax is not specifically known. It can be assumed by inspection that the wax has a smaller elastic modulus than the cement and the cement smaller than the cantilevered beam. For this reason, we cannot expect the theoretical results from the pin-force model to be accurate for attachment techniques involving these materials.

5.2.2 Differences in Authority due to Removing the Actuator

In observing the change in authority due to removal of the actuator, some attachment techniques exhibited the greatest change in authority at some modes while not at others.

A summary of these results is listed in Table 5.2.5. These numerical values correspond to the slope calculated from a linear, least squares curve fit of the authority as a function of removals from the beam. Figures 5.2.5 through 5.2.9 illustrate the magnitude of the frequency response function for each removal from the beam normalized with respect to the first application of the actuator. These plots are made for modes two through six of the attachment technique involving a piezoelectric actuator attached to a stiffener with cement and the stiffener to the beam with wax.

Table 5.2.4. Removal Reduction for Each Mode of Vibration (G's/volt/removal, dB)

Bonding Technique	mode 2	mode 3	mode 4	mode 5	mode 6
piezoelectric actuator, cement, stiffener, cement, beam	-0.479	-0.665	0.178	-0.178	-0.535
piezoelectric actuator, cement, stiffener, wax, beam	-0.235	-0.208	-0.649	-0.474	-0.101
piezoelectric actuator, wax, beam	-0.112	-0.081	0.009	0.027	0.217

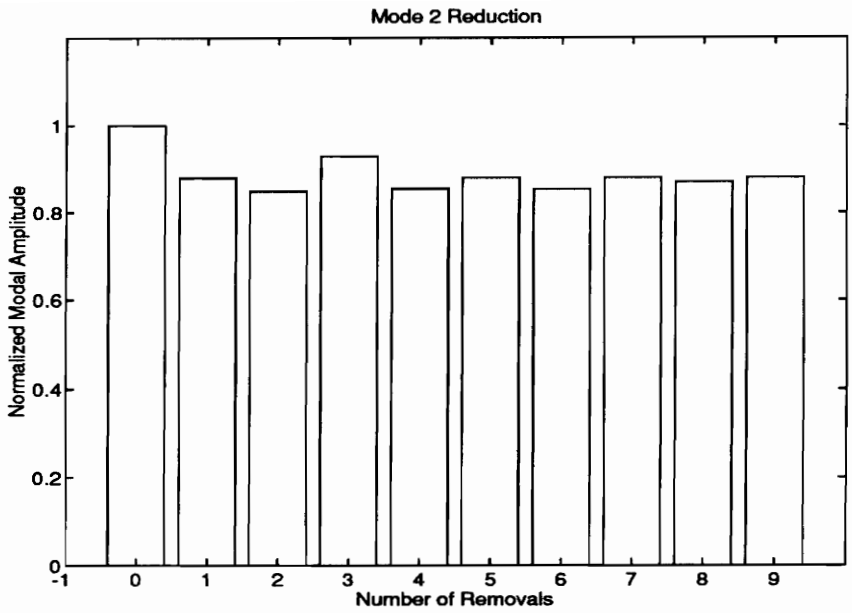

Figure 5.2.5. Normalized Modal Amplitude of the Second Mode of the Piezoelectric Actuator, Cement, Stiffener, Wax, Beam, Attachment Technique

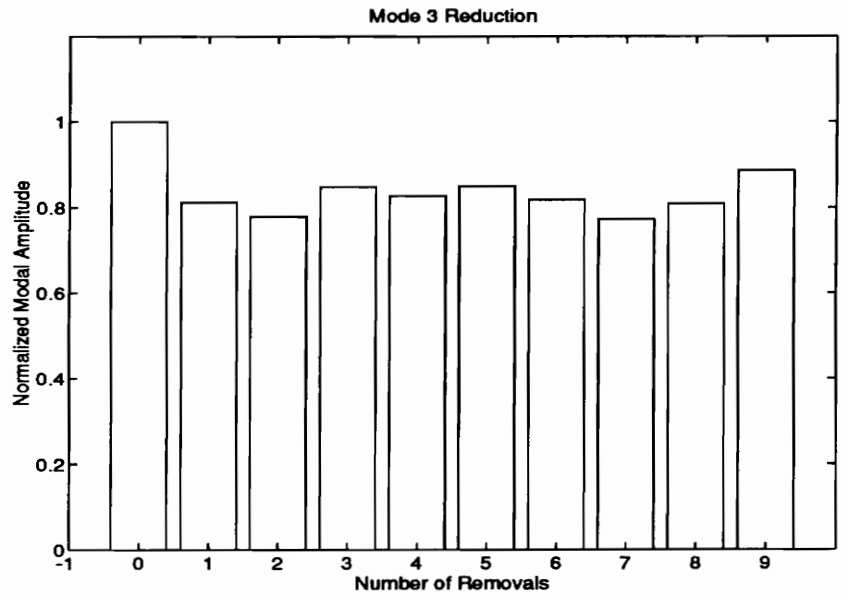

Figure 5.2.6. Normalized Modal Amplitude of the Third Mode of the Piezoelectric Actuator, Cement, Stiffener, Wax, Beam, Attachment Technique

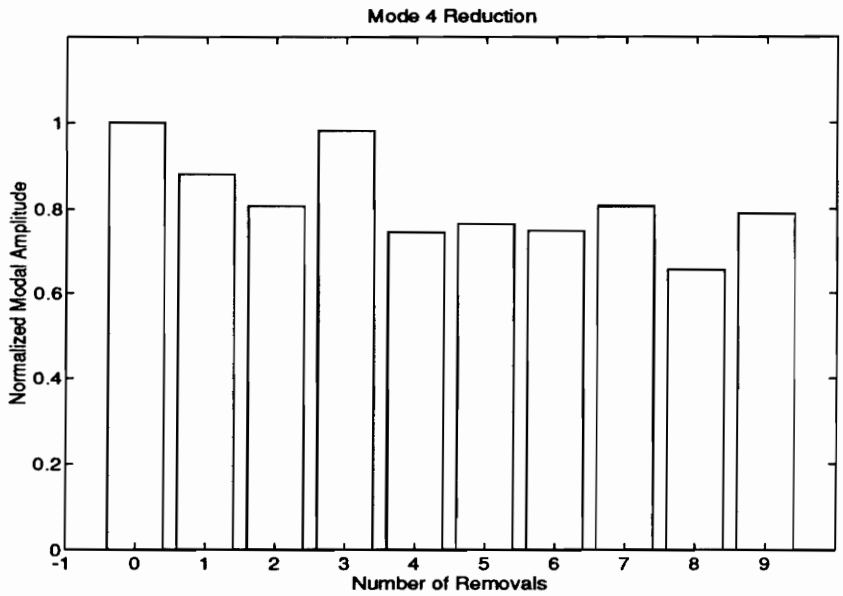

Figure 5.2.7. Normalized Modal Amplitude of the Fourth Mode of the Piezoelectric Actuator, Cement, Stiffener, Wax, Beam, Attachment Technique

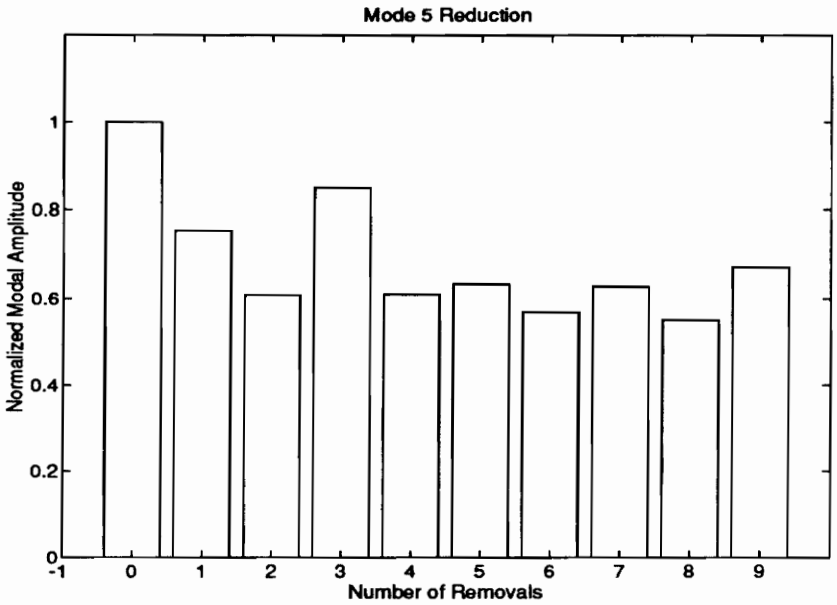

Figure 5.2.8. Normalized Modal Amplitude of the Fifth Mode of the Piezoelectric Actuator, Cement, Stiffener, Wax, Beam, Attachment Technique

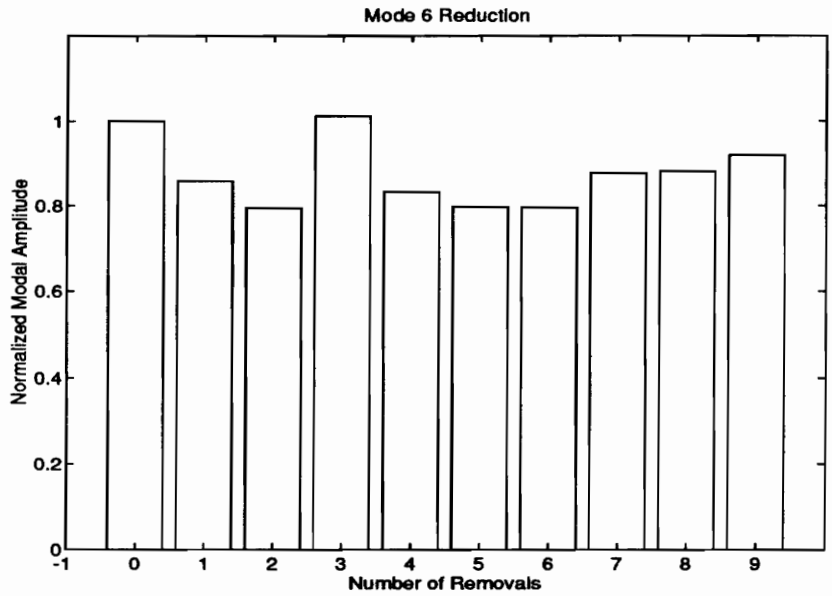

Figure 5.2.9. Normalized Modal Amplitude of the Sixth Mode of the Piezoelectric Actuator, Cement, Stiffener, Wax, Beam, Attachment Technique

Removing the actuator from the beam changed the authority of the actuator, but the change was not monotonic. The non-monotonic change suggests that removing the actuator does not progressively damage the piezoelectric actuator. Instead, the damage, if any, is random.

The overall authority reduction for the former attachment technique was no less than seventy percent of the first application for modes two, three, and six. For modes four and five, the reduction was no less than fifty percent. Normalized plots of the change in authority for the other attachment techniques are located in Appendix B.

5.3 Changes in Damping Ratios

Constructing a removable, reusable actuator involves adding to the permanent attachment technique different, and in some cases extra, bonding layers to the piezoelectric actuator. The addition of more bonding layers changes the physical parameters of the system; therefore, each attachment technique will have different damping ratios. The numerical differences in the damping ratios are discussed in this section.

5.3.1 Differences in Damping Ratios due to Different Attachment Techniques

The damping ratios for the first application of each attachment technique were calculated using a single degree of freedom curve fit through the third mode. The third mode was chosen in order to narrow the scope of the observation and because it exhibited few closely spaced modes and had small confidence intervals. The attachment technique that involved a piezoelectric actuator cemented to the beam had the smallest damping ratio of all the attachment techniques. The attachment technique that involved a piezoelectric actuator attached to a stiffener with cement and the stiffener to the beam with wax had the highest damping ratio. The values of the sample mean of the damping ratios and their respective 95% confidence intervals are listed in Table 5.3.1 These values correspond to the first application to the structure.

Table 5.3.1 Damping Ratios of Each Attachment Technique for the First Application

Attachment Technique	Damping Ratio Sample Mean (%)
piezoelectric actuator, cement, beam	1.619 ± 0.064
piezoelectric actuator, cement, stiffener, cement, beam	1.907 ± 0.021
piezoelectric actuator, cement, stiffener, wax, beam	2.015 ± 0.064
piezoelectric actuator, wax, beam	1.796 ± 0.044

The attachment techniques that involved a stiffener had higher damping ratios than those that did not. The attachment techniques that involved wax had higher damping ratios than a similar attachment technique that involved cement. The end result was that adding extra bonding layers to the permanent attachment technique or using wax instead of cement increased the damping ratio through the third mode.

5.3.2 Differences in Damping Ratios due to Removing the Actuator

The damping ratios were also calculated for each removal from the structure. In order to observe the change in the damping ratio due to removal from the structure, a linear least squares curve fit was performed. The slope of this line represented the change in damping ratio as a function of the removals from the structure. The slopes of the linear, least squares curve fit are small, which signifies negligible change in damping ratio as the actuator is removed from the structure. Table 5.3.2 contains the values of the slope of the linear, least squares curve fit, and Figure 5.3.1 contains plots of the calculated damping ratios and the linear, least squares curve fit. Therefore, removing the actuator from the

structure does not significantly change the damping ratio of the frequency response between the actuator and the structure.

5.3.2. Slope of Linear, Least Squares Curve Fit of Damping Ratios

Attachment Technique	Slope (damping ratio/removal)
piezoelectric actuator, cement, stiffener, cement, beam	0.0040
piezoelectric actuator, cement, stiffener, wax, beam	0.0191
piezoelectric actuator, wax, beam	-0.0002

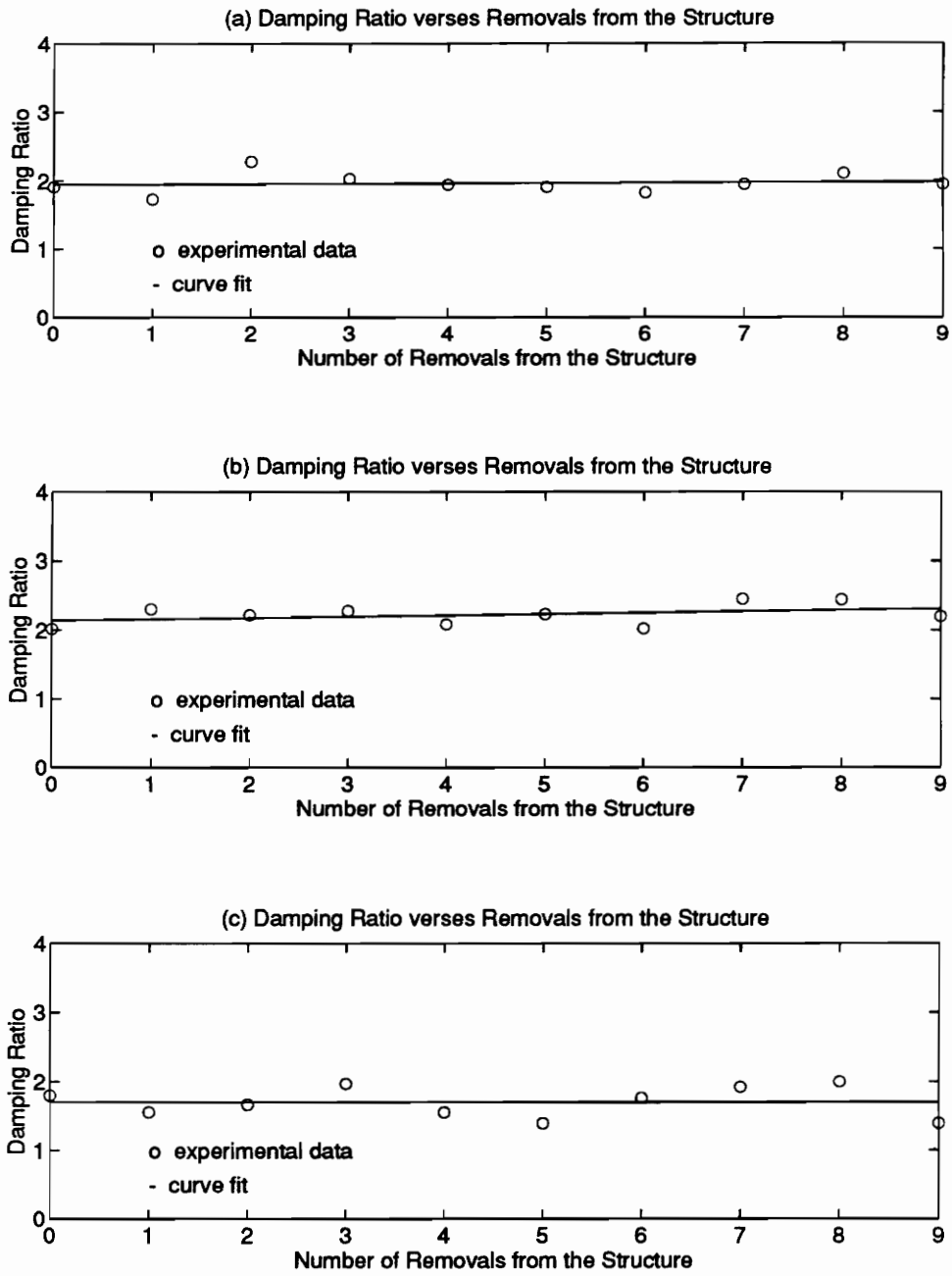

Figure 5.3.1. Damping Ratios as a Function of Removals from the Structure for:
(a) piezoelectric actuator, cement, stiffener, cement, beam
(b) piezoelectric actuator, cement, stiffener, wax, beam
(c) piezoelectric actuator, wax, beam

5.4 Ease of Use of the Removable, Reusable Piezoelectric Actuators

The following qualitative observations have been made about the actuators with regard to their usability, durability, and authority. The piezoelectric actuator attached to the host structure with cement had high authority when compared with the other actuators. It was also easy to apply to the host structure, but the attachment was not removable.

The piezoelectric actuator attached to a stiffener and the stiffener to the host structure both with cement had a medium authority level as compared to the other attachment techniques. This attachment technique had a medium authority reduction as compared to the other removable attachment techniques. It was easy to apply but difficult to remove. The removal process involved large deformations to the piezoelectric actuator, and as a result, there was a small but probable tendency of the piezoelectric actuator to break during removal. Cleaning the old cement from the surface of the stiffener before the next application was a difficult and tedious task.

The piezoelectric actuator attached to a stiffener with cement and the stiffener to the host structure with wax had a medium authority level as compared to the other attachment techniques. This attachment technique had the least amount of authority reduction. It was easy to apply and easy to remove. The removal process involved no significant deformation to the piezoelectric actuator, and thus there was no breakage. In addition to this, cleaning the surface of the stiffener was an easy task.

greatest authority reduction. The piezoelectric actuator was easy to apply and remove, but it was difficult to handle without breaking.

5.5 Inappropriate Use of an Electromagnetic Shaker to Resemble a Piezoelectric Actuator

Since no previous work has been conducted in the area of removable, reusable actuators, several removable actuator attachment techniques were considered for predicting the dynamic response of a permanently attached piezoelectric actuator. One such actuator was an electromagnetic shaker. This section describes the effectiveness of using an electromagnetic shaker to predict the dynamic response of a permanently attached piezoelectric actuator.

The electromagnetic shaker did not adequately represent a permanently attached piezoelectric actuator. The shaker had eight modes of vibration from 0 to 2000 Hz, whereas the piezoelectric actuator had only six (see Figs. 5.5.1 and 5.5.2). The removable, reusable piezoelectric actuators, on the other hand, resembled more closely the dynamic response of the permanently attached piezoelectric actuator. This can be seen by comparing the frequencies of the second, third, and fourth modes of vibration of the removable, reusable piezoelectric actuators to the permanent piezoelectric actuator (refer to Figs. 5.1.1 through 5.1.4). The difference in frequency between the second mode of the electromagnetic shaker and the permanent piezoelectric actuator was 15 Hz, whereas the difference in frequency for each removable, reusable actuator was at most 5 Hz. The difference in frequency between the third mode of the electromagnetic shaker and the permanent piezoelectric actuator was 55 Hz, and the difference in frequency for each

removable, reusable actuator was at most 25 Hz. For the fourth mode, the difference in frequency between the electromagnetic shaker and the permanent piezoelectric actuator was 90 Hz, while the difference in frequency for each removable, reusable actuator was at most 45 Hz. This trend continues throughout the rest of the modes of vibration.

The electromagnetic shaker did not have any antiresonances between 0 and 2000 Hz. For the permanently attached piezoelectric actuator in Fig. 5.2.2, there is an antiresonance that occurred around the fourth mode of its frequency response function.

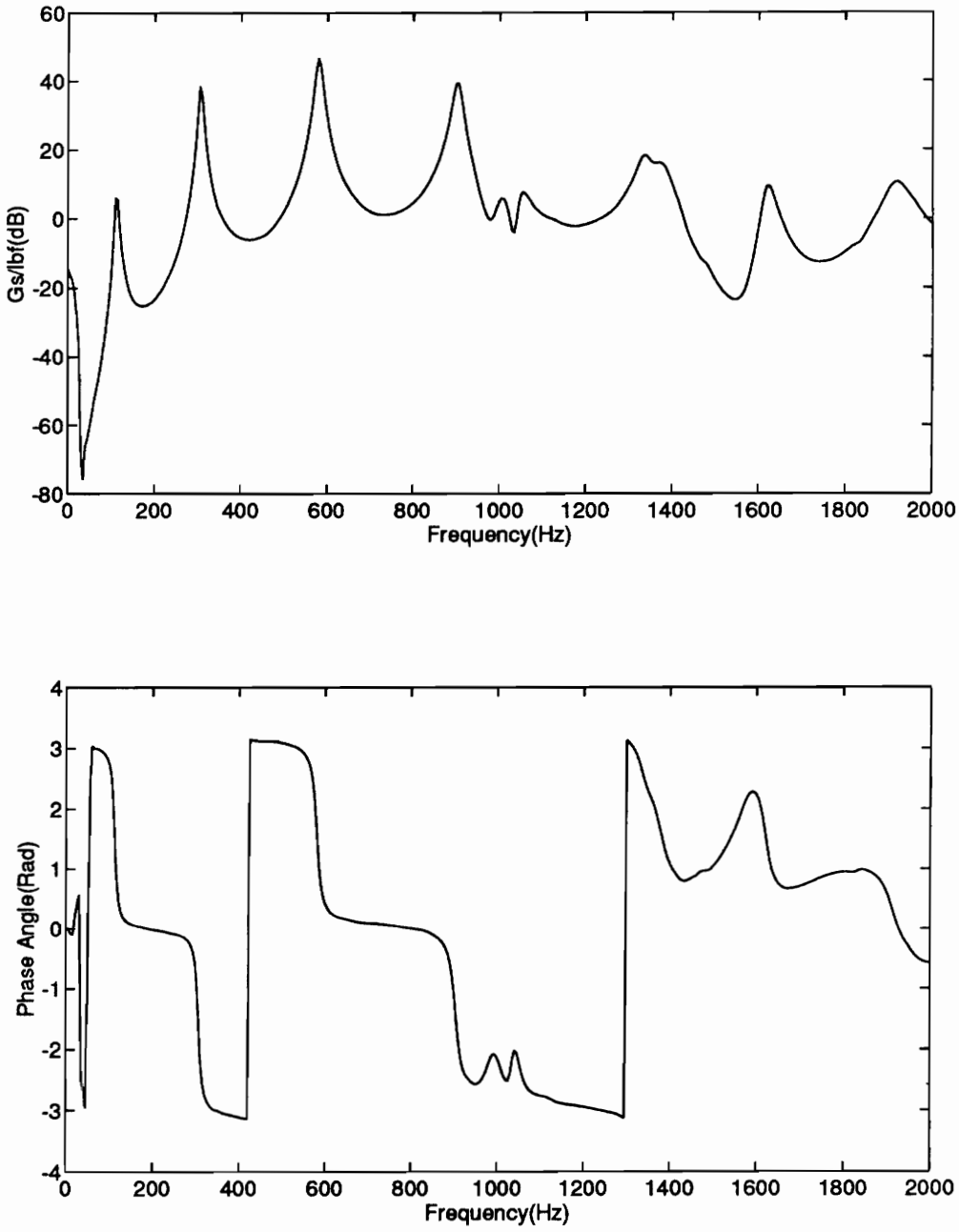

Figure 5.5.1. Frequency Response Function Between an Electromagnetic Shaker and a Cantilevered Beam

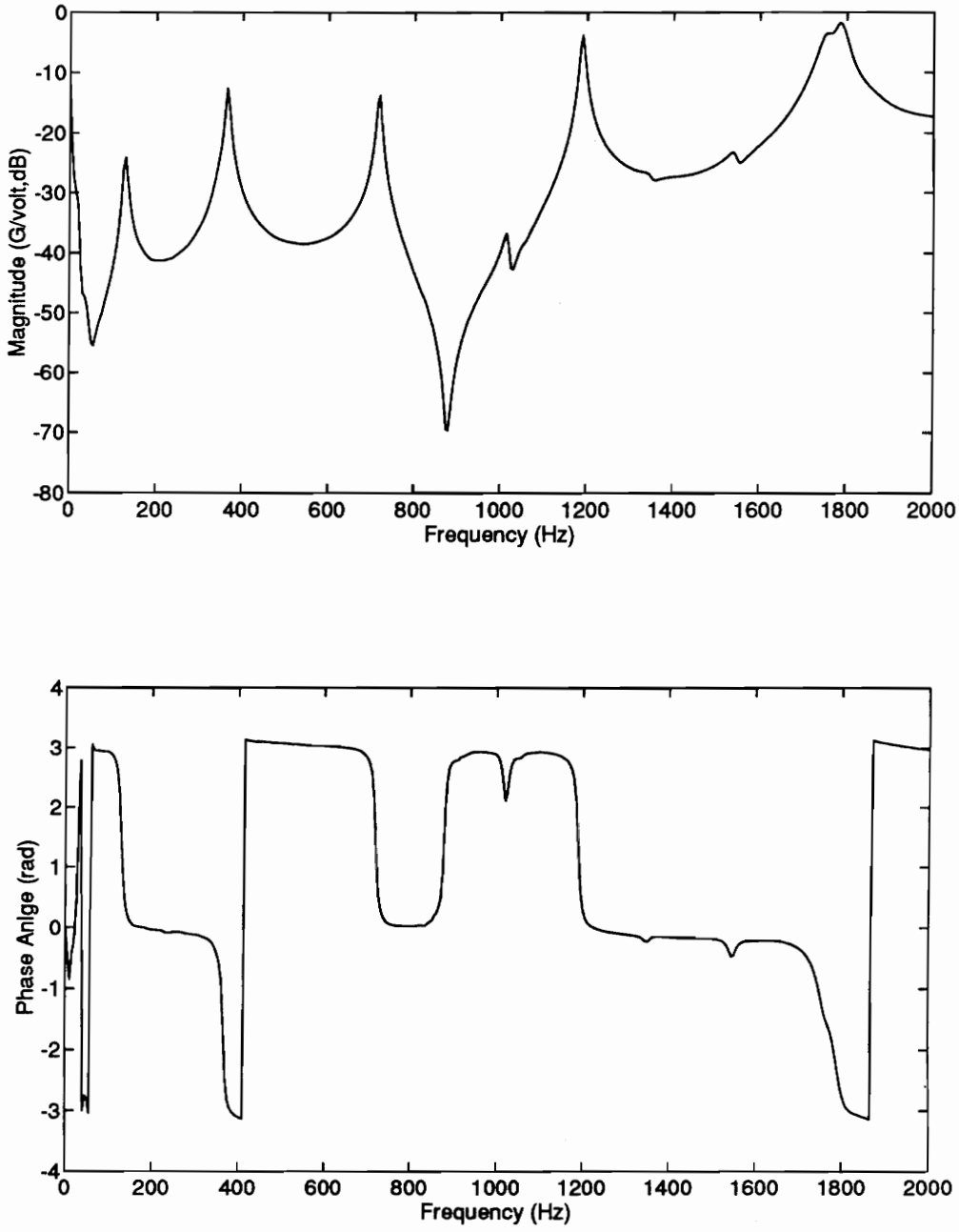

Figure 5.5.2. Frequency Response Function Between a Permanently Attached Piezoelectric Actuator and a Cantilevered Beam

5.6 Poor Coherence at Low Frequencies

The coherence values were low in the region of low frequencies of the frequency response function. The poor coherence can be attributed to several factors. One factor is that piezoelectric actuators do not actuate well at low frequencies. This poor performance will produce responses that are close to the noise floor of the measuring devices, thus resulting in low coherence. Another factor is that a burst random test has the potential of obtaining a new sample before the response from the previous sample has diminished. This would also supply uncorrelated signal content in the output response of the lower frequencies, thus resulting in low coherence. The frequencies at which the sample mean of the coherence first exceed 0.95 are stated in Table 5.6.1. These values are stated for the first application of each attachment technique.

Table 5.6.1. Frequencies at which the Sample Mean of the Coherence Exceeds 0.95

Attachment Technique	Frequency (Hz)
piezoelectric actuator, cement, beam	95
piezoelectric actuator, cement, stiffener, cement, beam	90
piezoelectric actuator, cement, stiffener, wax, beam	100
piezoelectric actuator, wax, beam	105

5.7 Shift of Antiresonance About Fourth Mode

The frequency response function of each attachment technique had one major antiresonance between 400 and 1000 Hz. This antiresonance always preceded the fourth mode of the frequency response function, with a few exceptions. There were some

instances where the antiresonance followed the fourth mode. Figure 5.7.1 illustrates this behavior for one actuator sample over two successive removals from the structure.

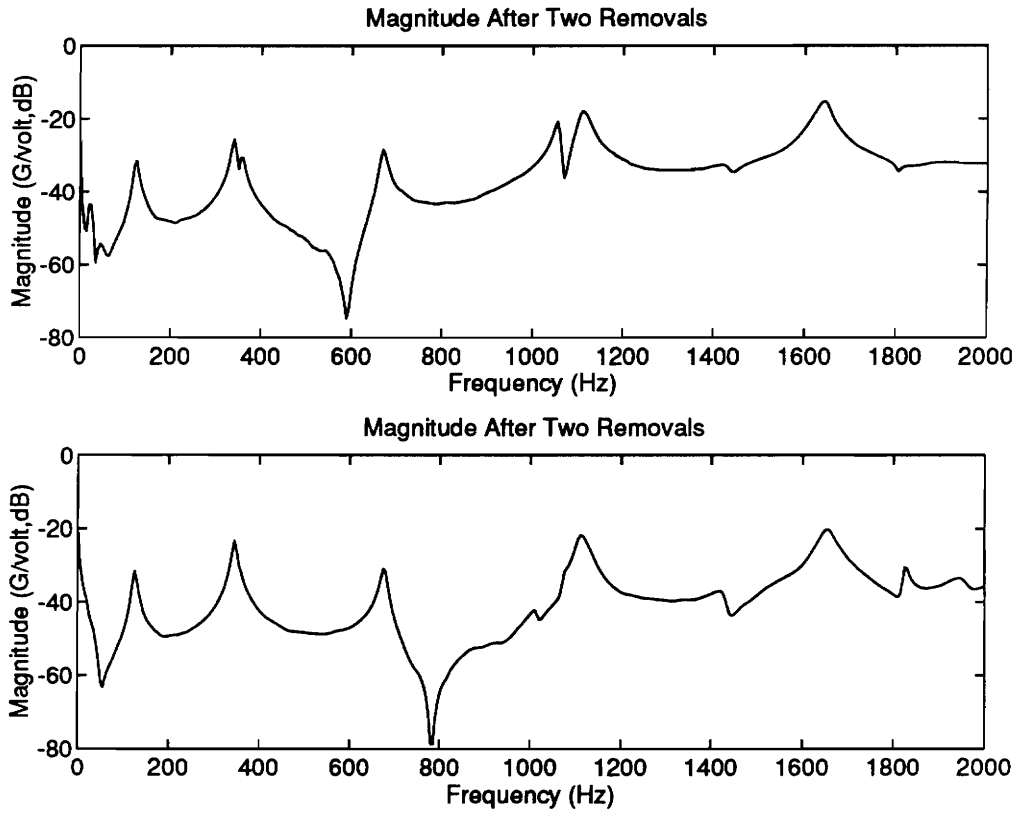

Figure 5.7.1. Piezoelectric Actuator, Cement, Stiffener, Cement, Beam, Attachment Technique with Antiresonance Before and After Fourth Mode

This sample is not an isolated case. Other samples also exhibited this behavior. Most of the samples that demonstrate this behavior belong to the attachment technique involving a piezoelectric actuator attached to the stiffener with cement and the stiffener to the host structure with cement. The attachment techniques that involve wax do not exhibit this behavior at all. Noting the presence of drift in some attachment techniques and not in others poses some questions as to the cause of this drift.

There are several aspects to the attachment of a piezoelectric actuator that can cause changes in the frequency response between the actuator and structure. One aspect is the position of the actuator. Changing the position of the actuator can change the characteristics of the frequency response function. It is possible that the attachment technique was not placed in the same position after removal. Although this is a possibility, it is not likely that position influences the drift in the antiresonance for these experiments. If this were a factor, then the drift would be seen in the other attachment techniques involving wax; they have as much probability to be mis-positioned as the others.

The greatest trend that supports the drift in the antiresonance is an unclean bonding surface. The only removable attachment technique that exhibited this behavior was the one where the piezoelectric actuator was attached to a stiffener with cement and the stiffener to the beam with cement. The first two samples that were tested did not have clean surfaces because care was not taken to clean the surfaces thoroughly. After proficiency with cleaning the bonding surface was attained, the remaining samples were cleaned thoroughly and they did not have the shift of the antiresonance about the fourth mode. This factor more than any other supports the cause of the drift of the antiresonance.

This observation manifests its importance when cleaning the structure surface would be impractical. Extraneous cement would be difficult to clean from a concave structure after the actuator is removed. In this case, an attachment technique involving wax would be more suitable for conducting tests that yield repeatable results.

5.8 Closing Remarks

The results of the theoretical and experimental data have been presented. The dynamic response characteristics of Chapter 3 have been discussed as well as some other areas of interest. These results will be summarized in the next and last chapter of this work.

CHAPTER 6
CONCLUSIONS AND FUTURE WORK

The objective of this research was to develop and construct three alternate techniques for bonding flat, piezoelectric patch-type actuators to structures. For each attachment technique, an analysis of the frequency response functions, actuation authorities, and damping ratios was conducted. This chapter outlines the conclusions of this work and future recommendations for further work.

6.1 Conclusions

The addition of different bonding layers changed the authority of the piezoelectric actuator. When comparing the authority level of one attachment technique to another, the order of increasing authority was different at different modes. In other words, some attachment techniques exhibited the greatest actuation authority over other attachment techniques at some modes but not at others.

The authority levels observed in the experimental data were different from the authority levels predicted from the pin-force model. The pin-force model was not an accurate model for the attachment techniques considered in this work because the assumption that plane sections remain plane was not accurate.

The authority of the actuators did change after removing the actuator from the structure. The change was not monotonically increasing or decreasing. In other words, removing

the actuator from the structure and reattaching it did not hinder or improve the authority of the piezoelectric actuators. For ten applications of each attachment technique, the authority reduction was no less that fifty percent of the original authority, and in most cases was no less than seventy percent.

When considering mode three of the frequency response functions of the different attachment techniques, the damping ratio was greater for attachment techniques that involved wax as opposed to cement. Similarly, attachment techniques that incorporated stiffeners had higher damping ratios as compared with those that did not incorporate a stiffener. The change in damping ratio did not significantly change as the actuator was reused.

Each attachment technique had its own unique advantages and disadvantages to its ease of use. The removable attachment technique that involved a stiffener cemented to the beam involved a great amount of strain when being removed. This attachment technique allowed greater authority from the piezoelectric actuator, but cleaning the structure and stiffener surface was difficult and time consuming. The attachment techniques involving wax were easy to remove, and the structure and stiffener surfaces were easy to clean. These attachment techniques did not allow as much authority from the piezoelectric actuator as those involving cement. The piezoelectric actuator used in the attachment technique involving wax without a stiffener had a high tendency to break when being removed and reattached to the beam.

The attachment technique that involved a piezoelectric actuator attached to a stiffener with cement and the stiffener attached to the beam with wax was the best estimator of the

permanent piezoelectric actuator. This attachment technique resembled the permanent authority as well as the other attachment techniques. This attachment technique also had the least authority reduction. Its only disadvantage was its wide confidence intervals.

Electromagnetic shakers do not make good predictors of piezoelectric actuator performance. The frequency response function from the electromagnetic shaker did not have an antiresonance from 0 to 2000 kHz, whereas the frequency response function from the piezoelectric actuator did. Also, the frequency of the modes for the electromagnetic shaker and piezoelectric actuator varied as much as 90 Hz.

The confidence intervals of the mean magnitude and phase angle of each attachment technique were largest in the areas containing antiresonance and closely spaced modes. The confidence intervals of the mean coherence were largest only in the regions containing antiresonance.

The coherence of the frequency response functions of the different attachment techniques was low for low frequencies. For each attachment technique, the sample mean of the coherence did not reach 0.95 until the frequency was between 90 and 105 Hz. Above this, the frequency response functions had good coherence except in regions of antiresonance.

The shift of the antiresonance from before the fourth mode to after the fourth mode was caused by an unclean bonding surface. This shift of antiresonance did not occur when the bonding surface was properly cleaned.

6.2 Future Work

Future work should include exploring different attachment techniques that are representative of the permanent actuator. These attachment techniques should be easy to apply and still prevent damage to the piezoelectric actuator. A more accurate model of the piezoelectric actuator and host structure interaction needs to be obtained so that the dynamic response of the host structure can be analytically predicted. Micro-measurements should be performed in order to observe trends that may alter the dynamic response characteristics of each attachment technique. Finally, the use of these removable and reusable actuators should move beyond simple structures to more complex structures where *ad hoc* approaches to experimental testing would be improved.

References

Beckwith, Thomas G., Roy D. Marangoni, and John H. Lienhard V. Mechanical Measurements, 5th ed., p. 70. Addison-Wesley, Reading, Massachusetts, 1993.

Beer, Ferdinand P. and E. Russell Johnston, Jr. Mechanics of Materials, pp. 153-155, 168-172. McGraw-Hill, New York, 1981.

Bendat, Julius S. and Allen G. Piersol. Random Data: Analysis and Measurement Procedures, 2nd ed., pp. 76-77. John Wiley and Sons, New York, 1986.

D'Cruz, Jonathan. "Active Control of Panel Vibrations with Piezoelectric Actuators," Journal of Intelligent Material Systems and Structures, vol. 4 no. 3, pp. 398-402, 1993.

Fuller, C.R., S.D. Snyder, C.H. Hansen, and R.J. Silcox. "Active Control of Interior Noise in Model Aircraft Fuselages Using Piezoceramic Actuators," AIAA Journal, vol. 39 no. 11, pp.2613-2617, 1992.

Han, Dr. Man Cheol. Software developed at Virginia Polytechnic Institute and State University, 1990.

Hanagud, S., M.W. Obal, and A.J. Calise. "Optimal Vibration Control by the Use of Piezoceramic Sensors and Actuators," Journal of Guidance, Control, and Dynamics, vol. 15 no. 5, pp. 1199-1206, 1992.

Hollkamp, Joseph J. "Multimodal Passive Vibration Suppression with Piezoelectrics," *Proceedings of the 34th Structures, Structural Dynamics, and Material Conference*, La Jolla, CA, 1993, pp. 3227-3233.

Lazarus, Kenneth B. and Edward F. Crawley. "Induced Strain Actuation of Composite Plates," GTL Report #197, Cambride, Massachusetts, 1989, pp. 17-26.

Levinson, Irving J. Statics and Strength of Materials, pp. 291-295. Prentice-Hall, New Jersey, 1971.

The Math Works Inc. Matlab, User's Guide. Natick, Massachusetts, 1993.

Palazzolo, A.B., et al. "Piezoelectric Actuator-Active Vibration Control of the Shaft Line for a Gas Turbine Engine Test Stand," American Society of Mechanical Engineers, paper 93-GT-262, pp. 1-12, 1993.

Shames, Irving H. Introduction to Solid Mechanics, pp. 177-183, 193-198. Prentice-Hall, New Jersey, 1975.

Walpole, Ronald E. and Raymond H. Myers. Probability and Statistics for Engineers and Scientists, 5th ed., pp. 413, 419-420. Macmillan, New York, 1993.

Wang, Bor-Tsuen, Ricardo A. Burdisso, and Chris R. Fuller. "Optimal Placement of Piezoelectric Actuators for Active Structural Acoustic Control," Journal of Intelligent Material Systems and Structures, 1994.

Appendix A

Figures A.1 through A.12 illustrate individual samples of the sample population for the frequency response functions. The frequency response functions are composed of the magnitude, phase angle, and coherence between the tip acceleration of the beam and the input voltage to the piezoelectric actuator. Only the first attachments of each attachment technique have been included in this appendix. These samples were combined with the other samples, according to the appropriate attachment technique, in order to calculate the confidence intervals.

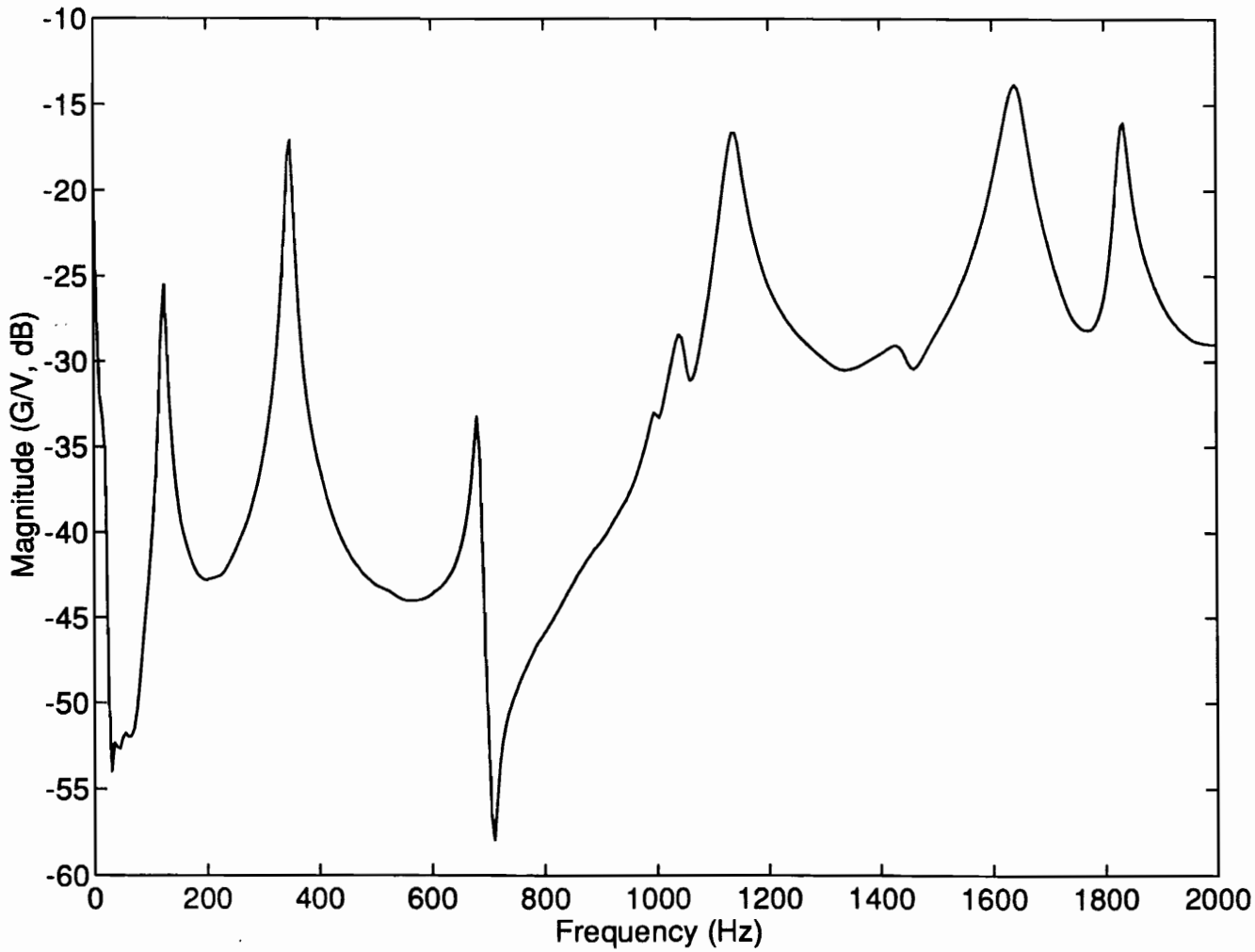

Figure A.1. Frequency Response Function Magnitude for the Piezoelectric Actuator, Cement, Beam Attachment Technique

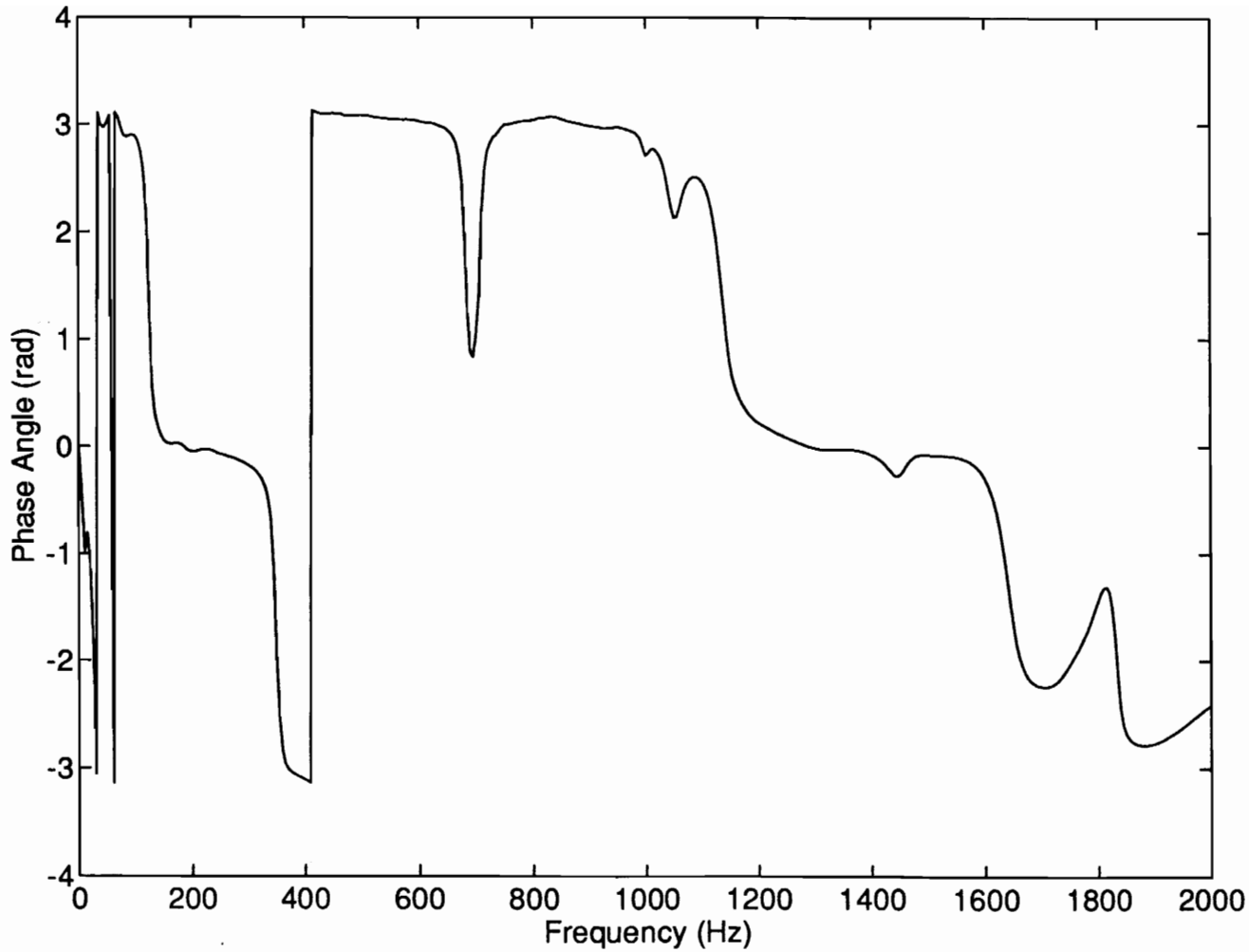

Figure A.2. Frequency Response Function Phase Angle for the Piezoelectric Actuator, Cement, Beam Attachment Technique

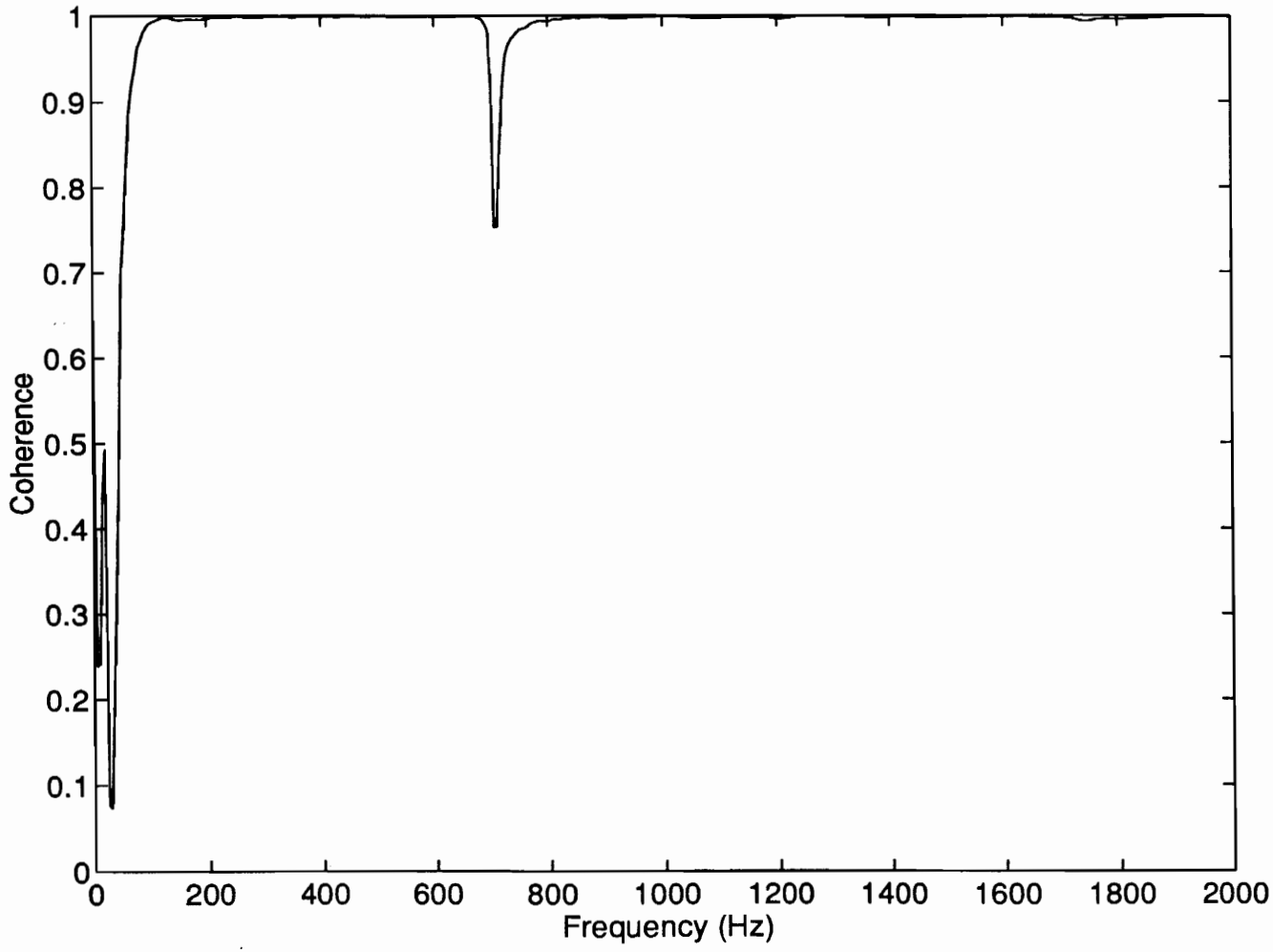

Figure A.3. Frequency Response Function Coherence for the Piezoelectric Actuator, Cement, Beam Attachment Technique

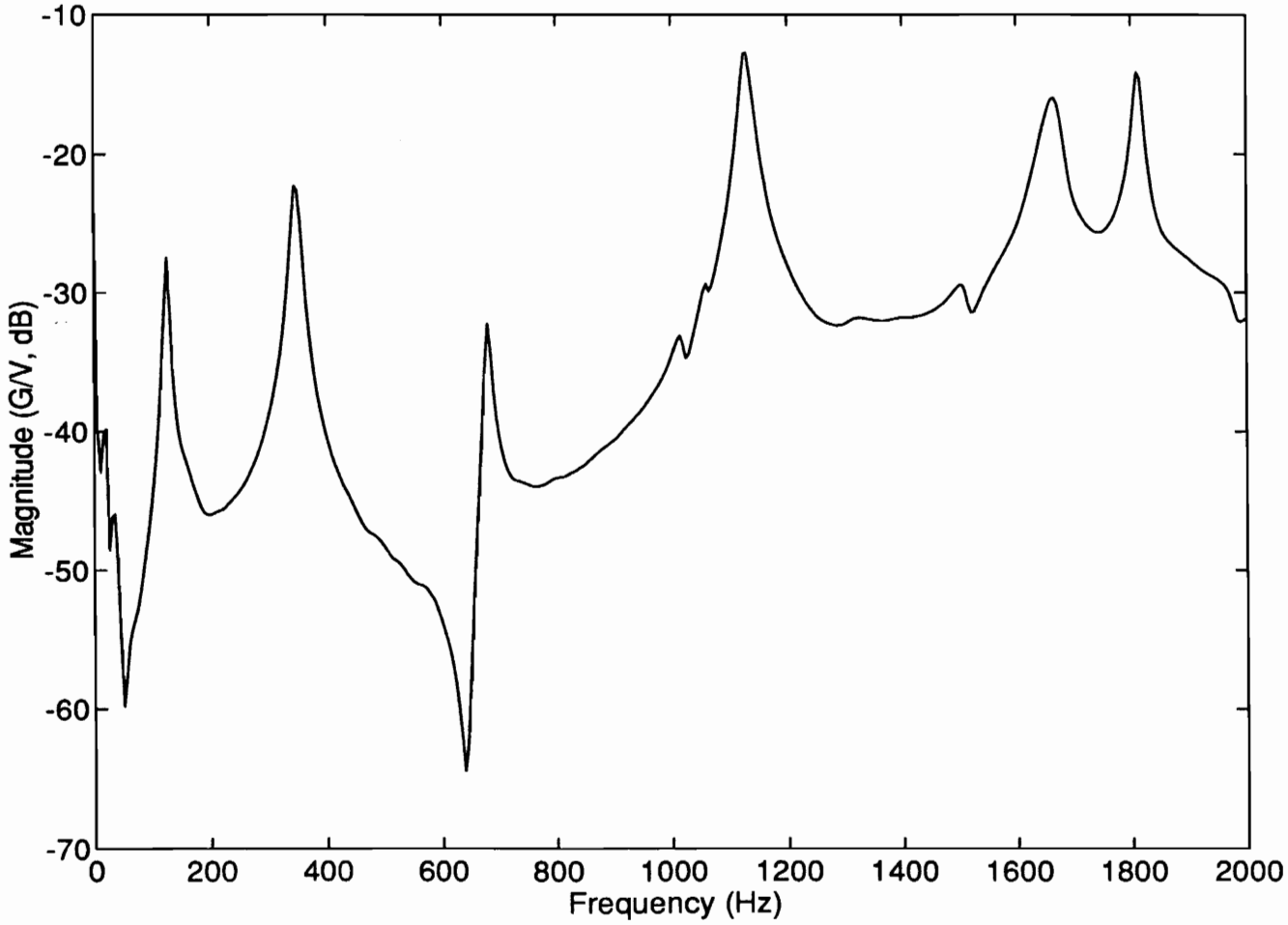

Figure A.4. Frequency Response Function Magnitude for the Piezoelectric Actuator, Cement, Stiffener, Cement, Beam Attachment Technique

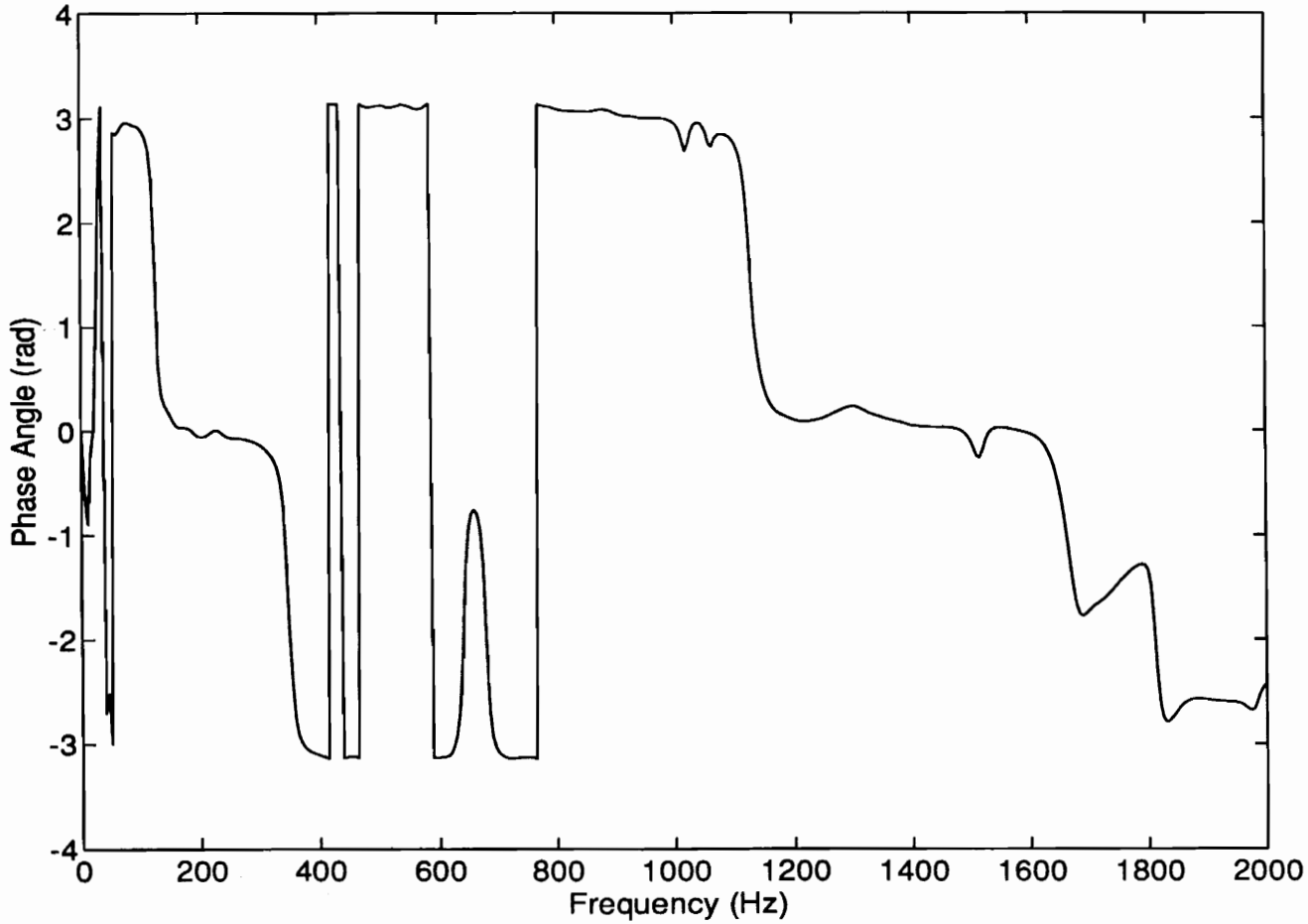

Figure A.5. Frequency Response Function Phase Angle for the Piezoelectric Actuator, Cement, Stiffener, Cement, Beam Attachment Technique

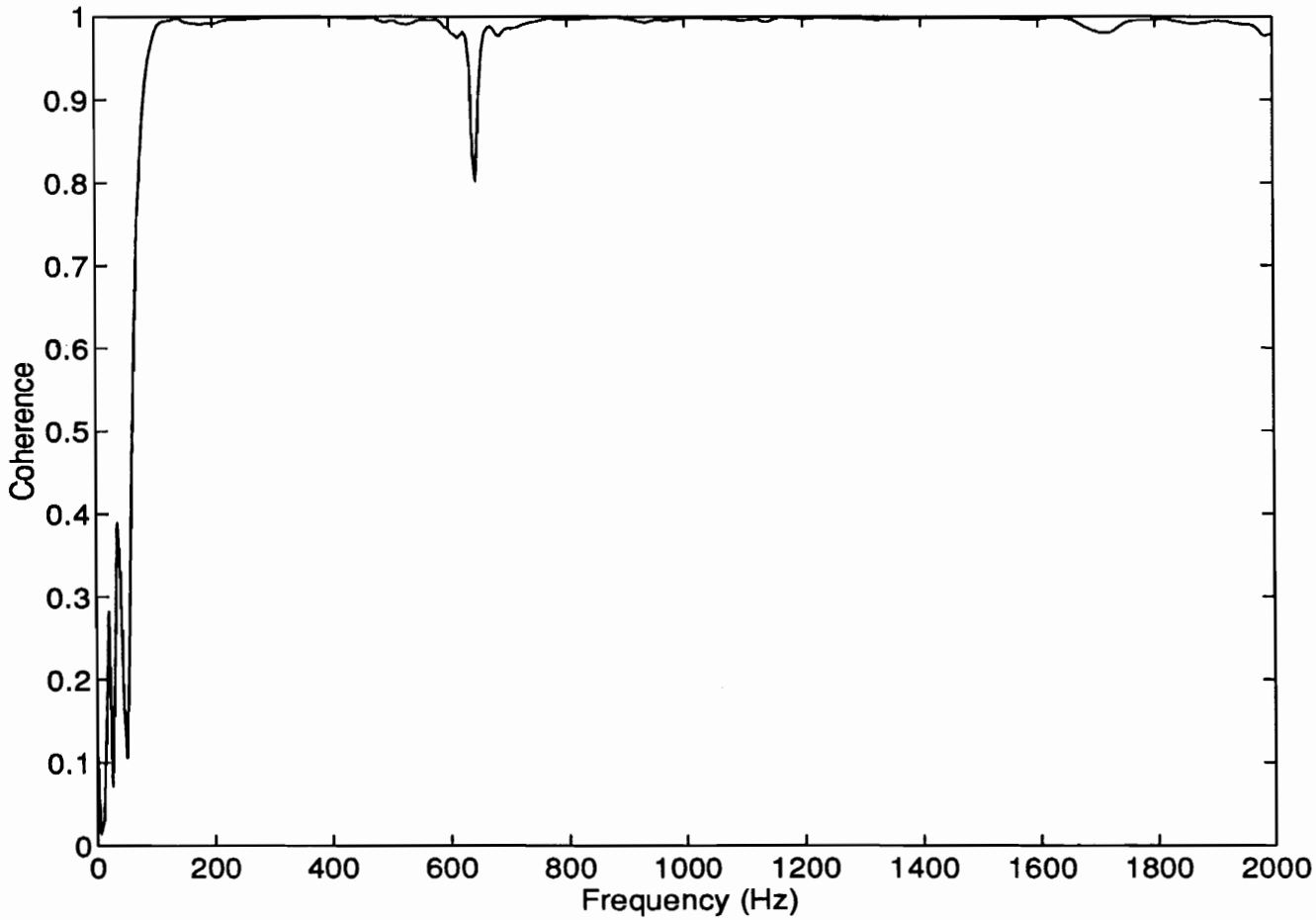

Figure A.6. Frequency Response Function Coherence for the Piezoelectric Actuator, Cement, Stiffener, Cement, Beam Attachment Technique

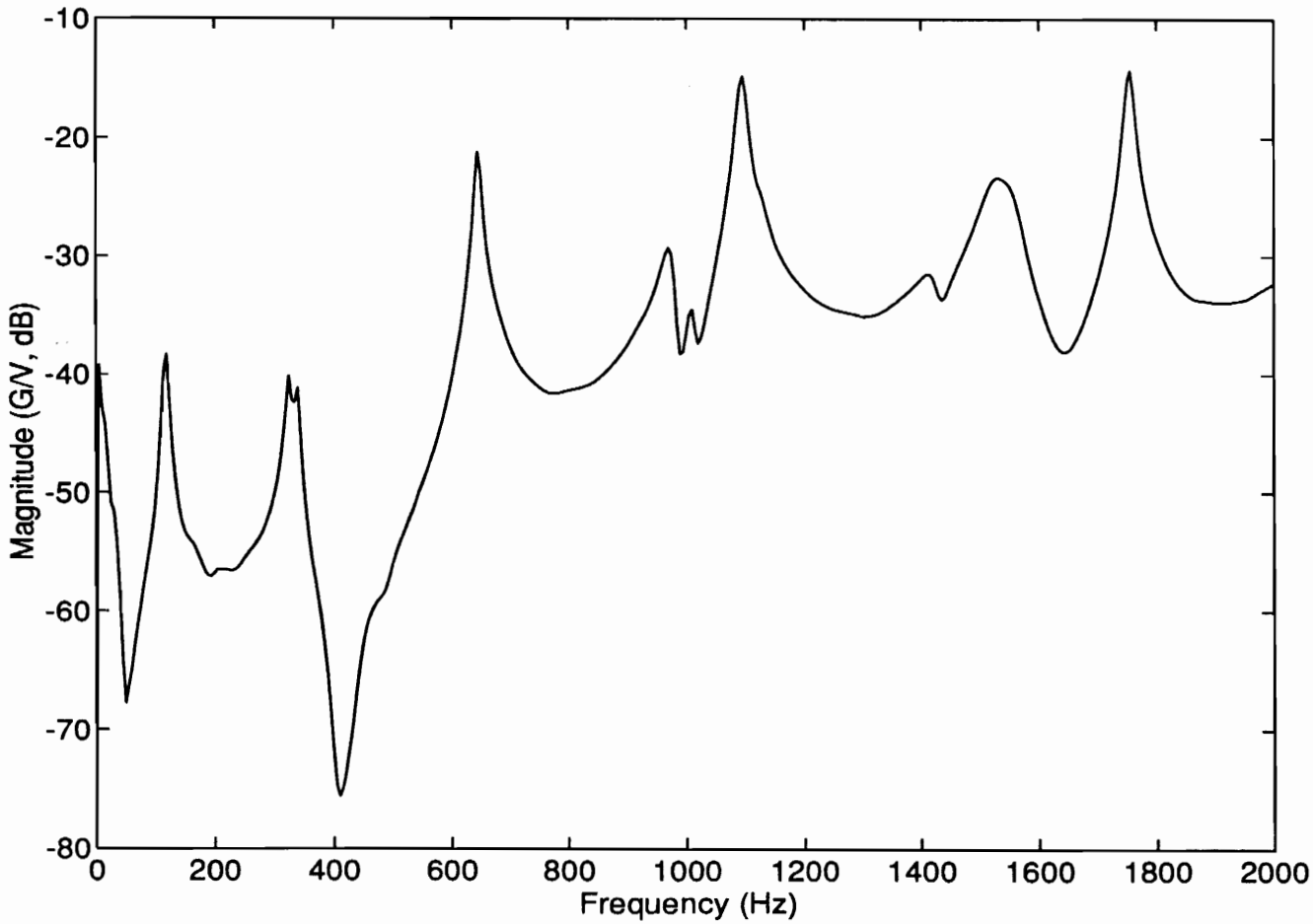

Figure A.7. Frequency Response Function Magnitude for the Piezoelectric Actuator, Cement, Stiffener, Wax, Beam Attachment Technique

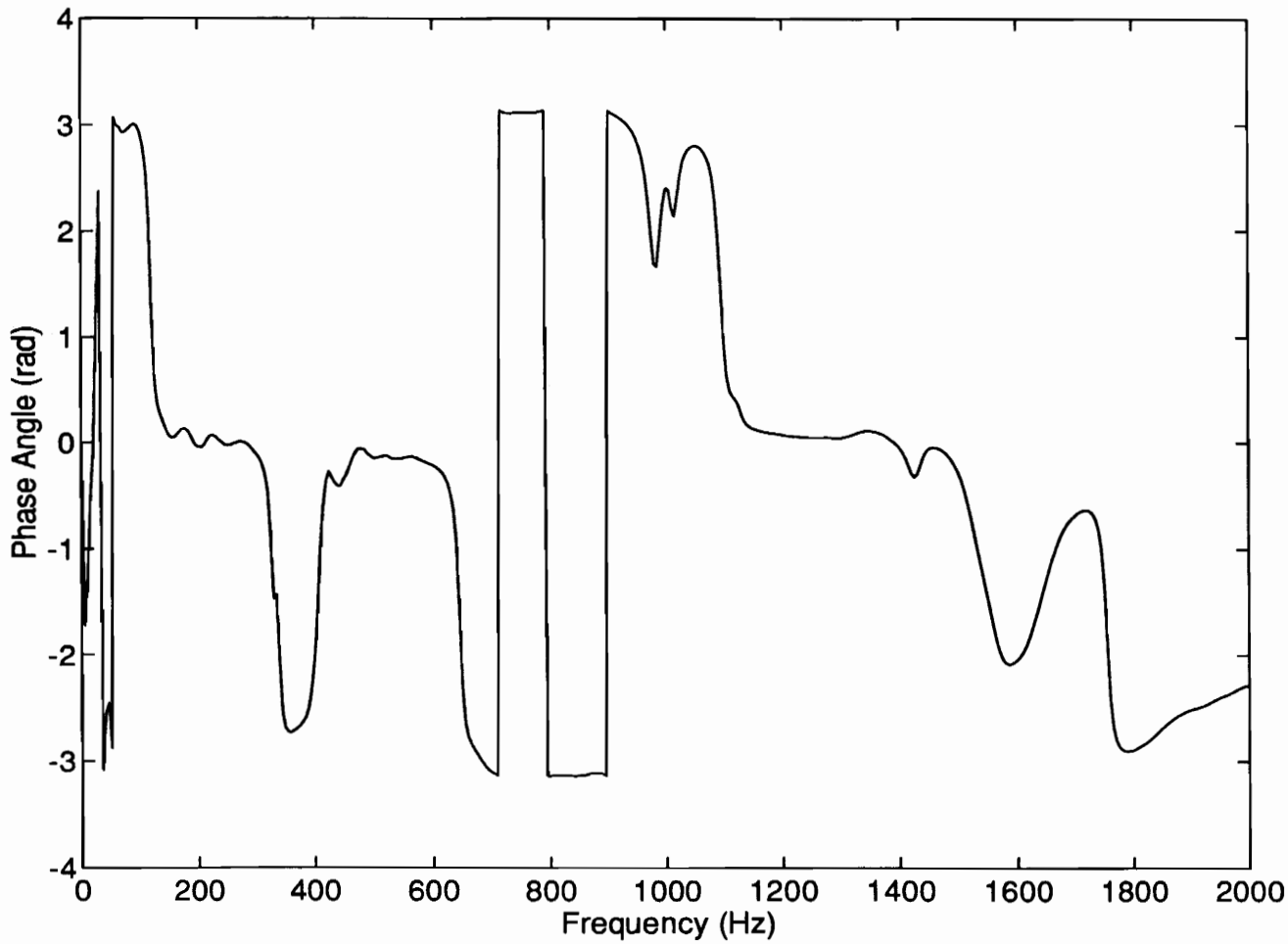

Figure A.8. Frequency Response Function Phase Angle for the Piezoelectric Actuator, Cement, Stiffener, Wax, Beam Attachment Technique

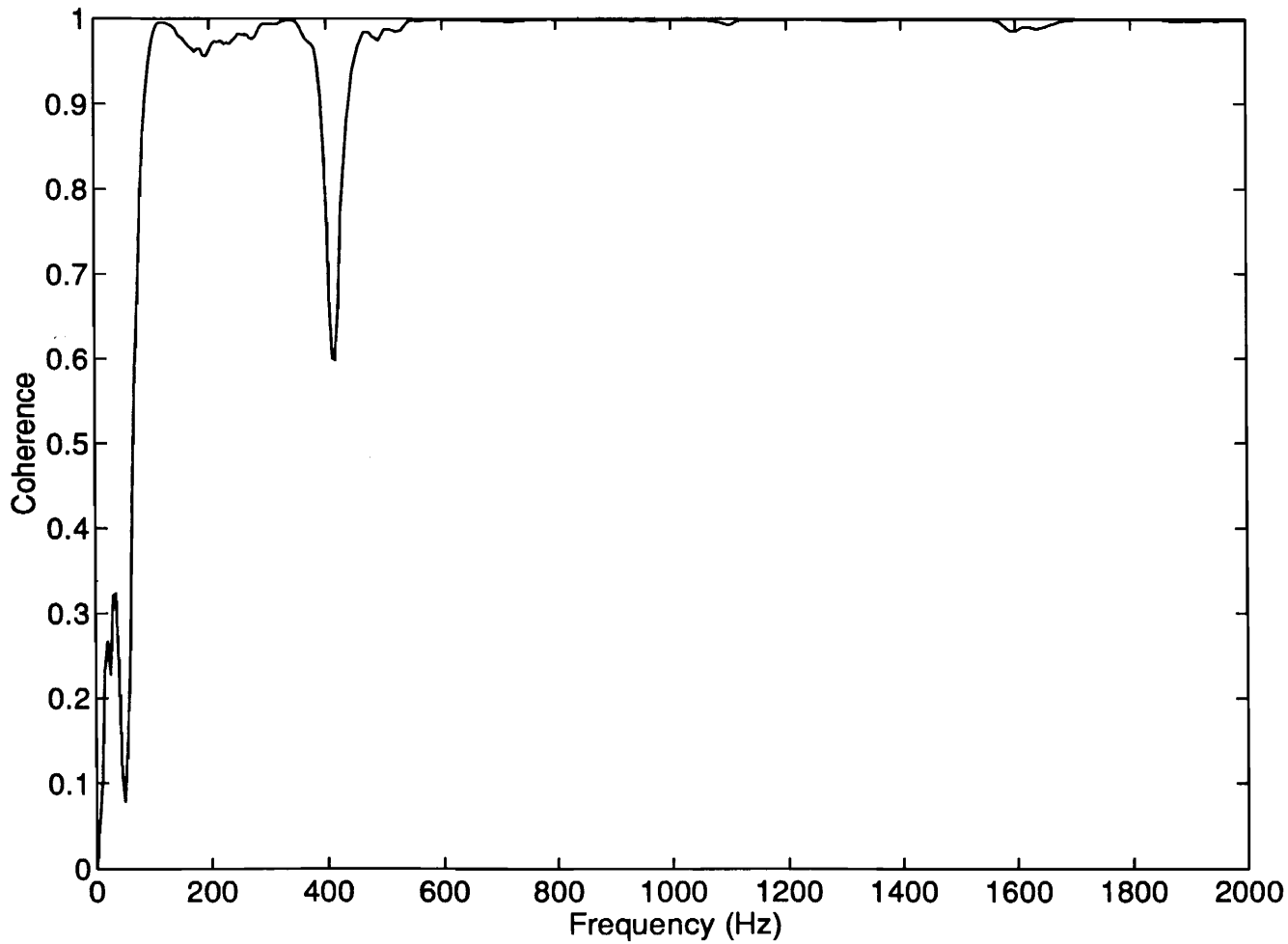

Figure A.9. Frequency Response Function Coherence for the Piezoelectric Actuator, Cement, Stiffener, Wax, Beam Attachment Technique

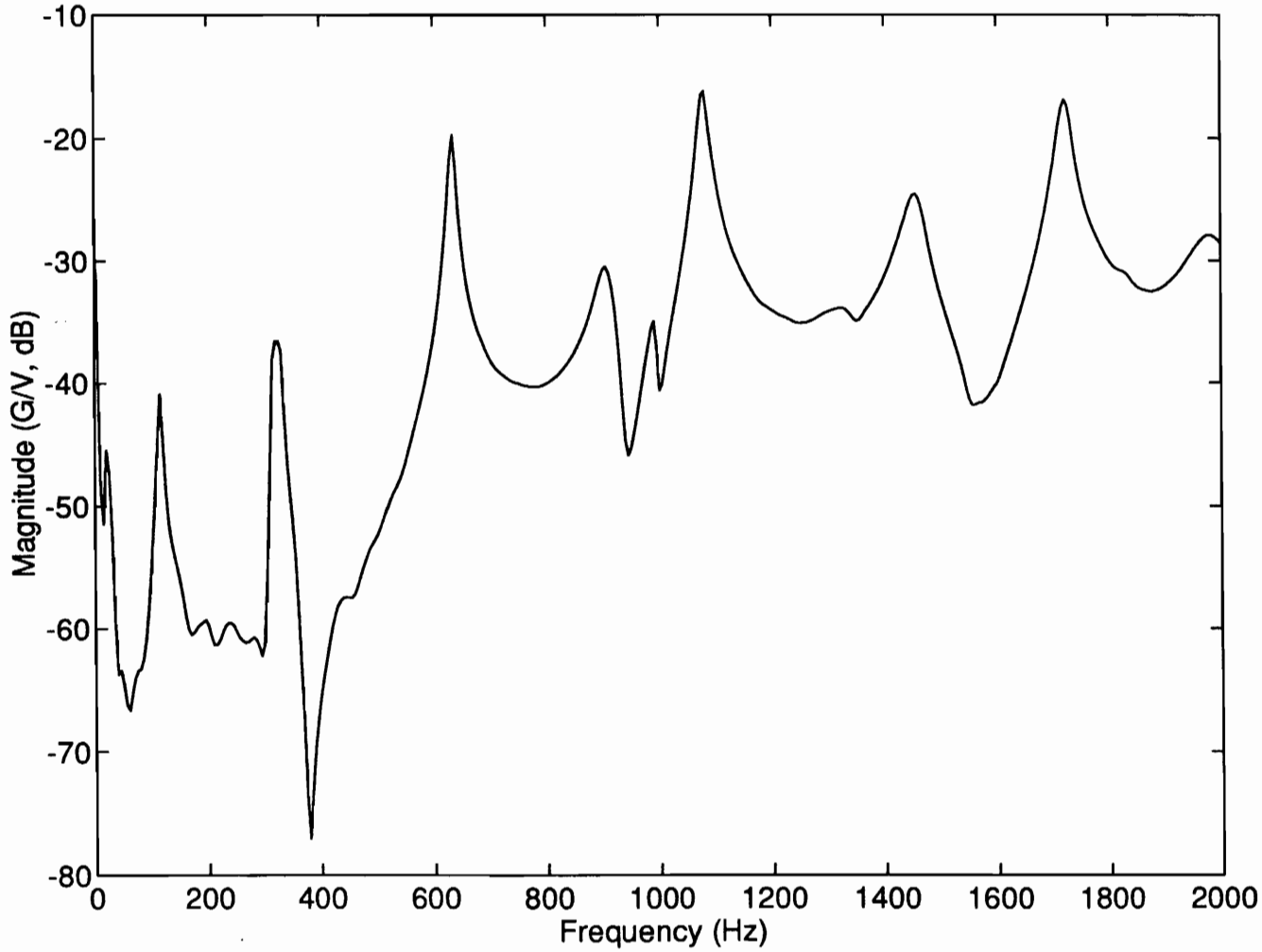

Figure A.10. Frequency Response Function Magnitude for the Piezoelectric Actuator, Wax, Beam Attachment Technique

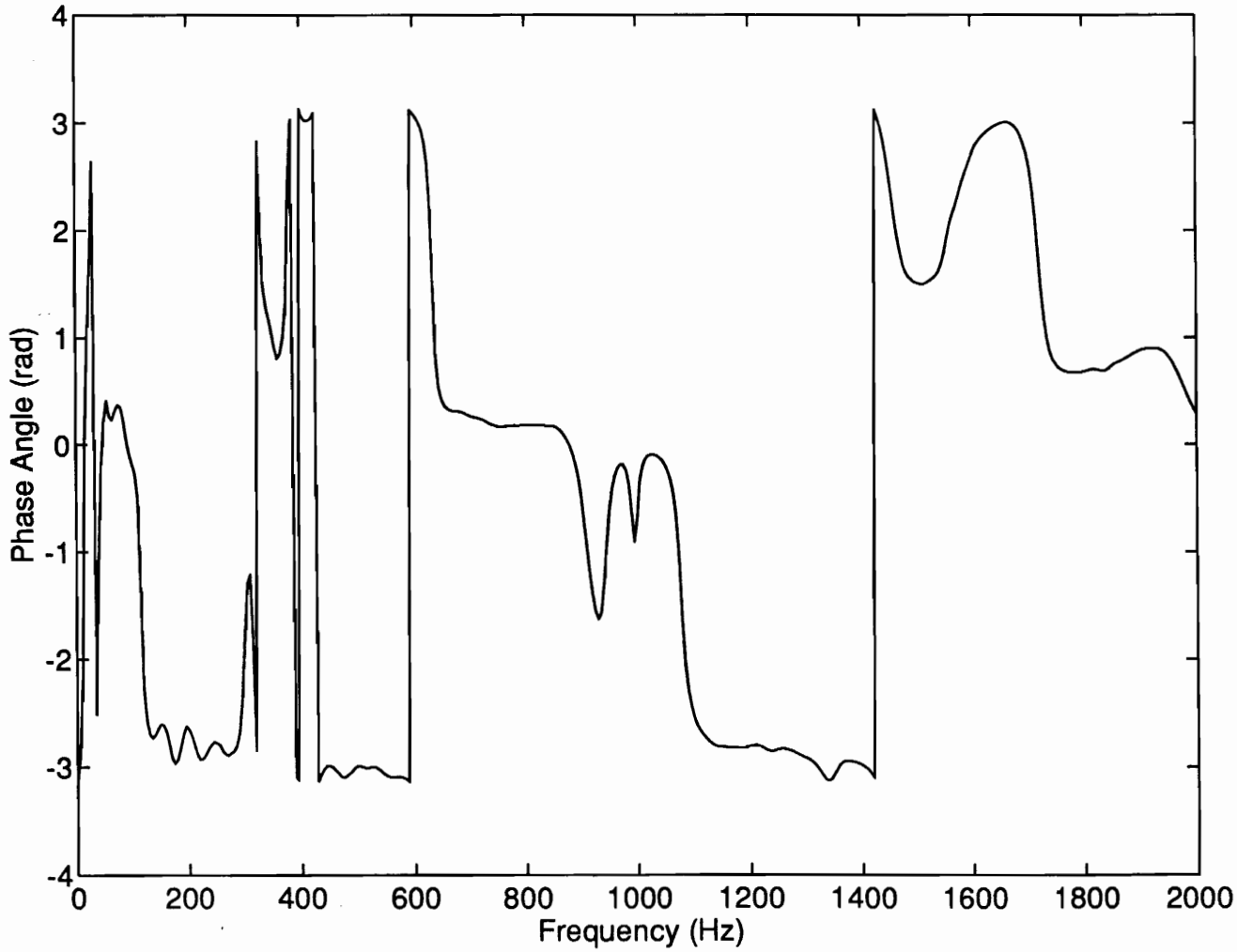

Figure A.11. Frequency Response Function Phase Angle for the Piezoelectric Actuator, Wax, Beam Attachment Technique

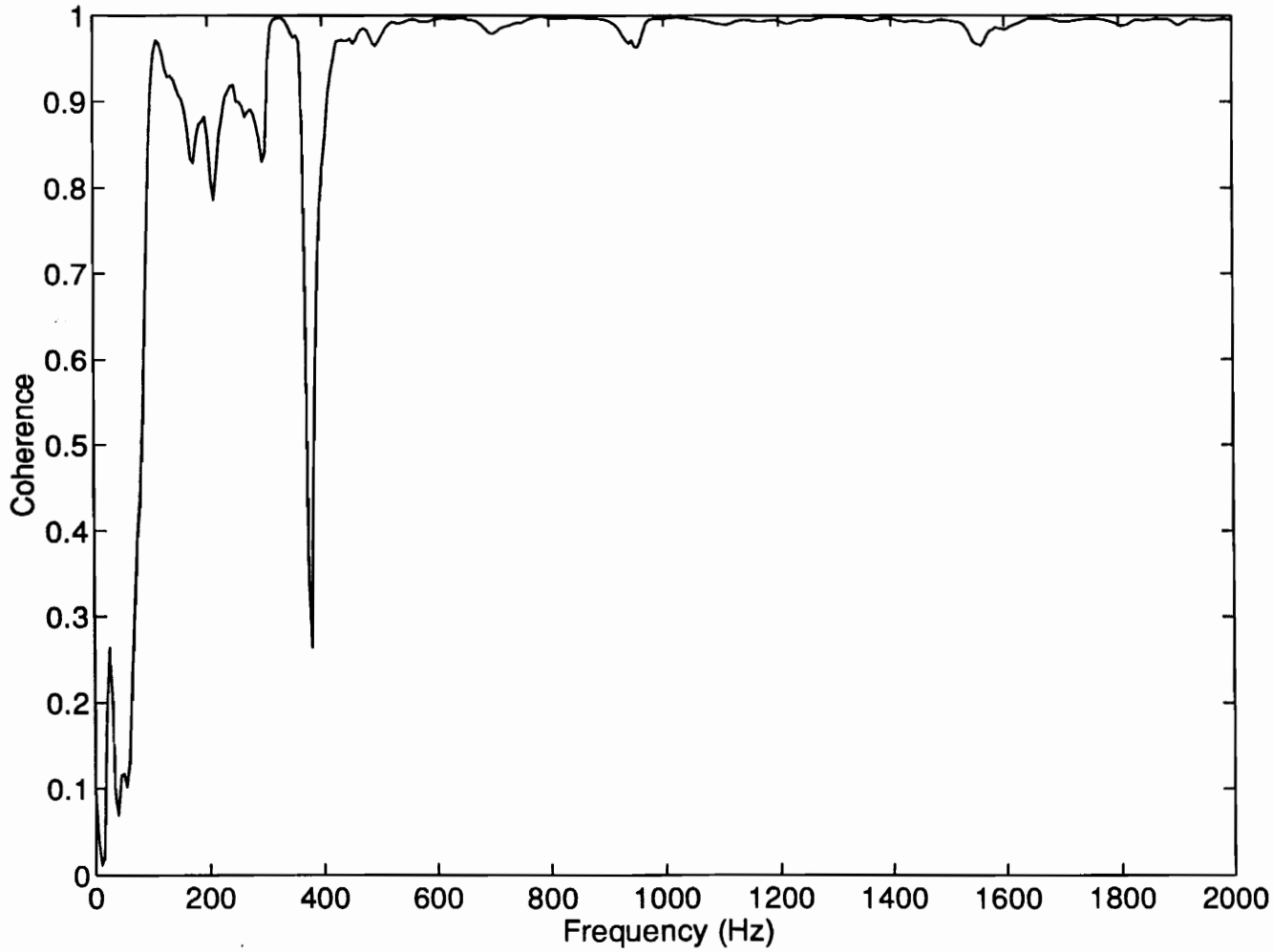

Figure A.12. Frequency Response Function Coherence for the Piezoelectric Actuator, Wax, Beam Attachment Technique

Appendix B

Figures B.1 through B.10 illustrate the magnitude of the frequency response function for each removal from the beam normalized with respect to the first application of the actuator. These plots are made for modes two through six for two attachment techniques, the first involving a piezoelectric actuator attached to a stiffener with cement and the stiffener to the beam with cement, and the second involving a piezoelectric actuator attached to the beam with wax. Chapter five contains the discussion of these plots as well as the figures containing the plots of the attachment technique involving a piezoelectric actuator attached to a stiffener with cement and the stiffener to the beam with wax.

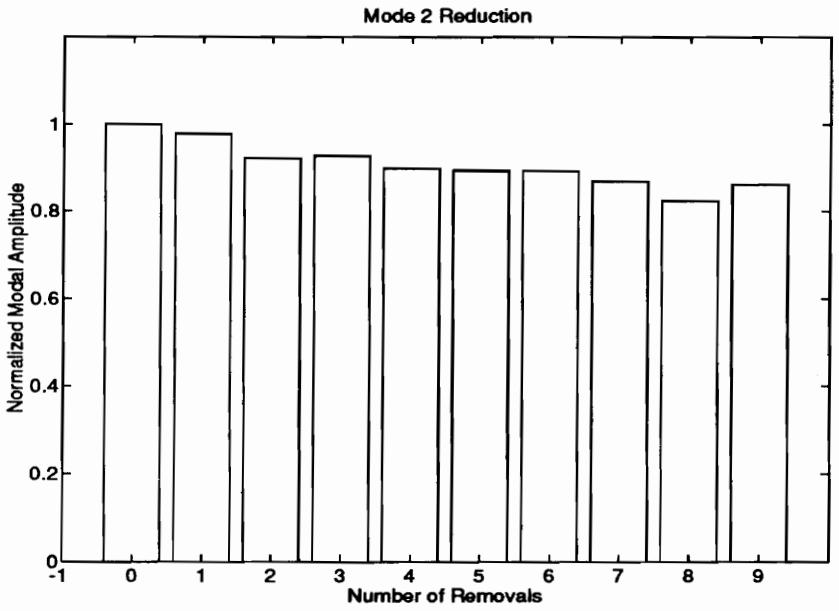

Figure B.1. Normalized Magnitude of the Second Mode of the Piezoelectric Actuator, Cement, Stiffener, Cement, Beam, Attachment Technique

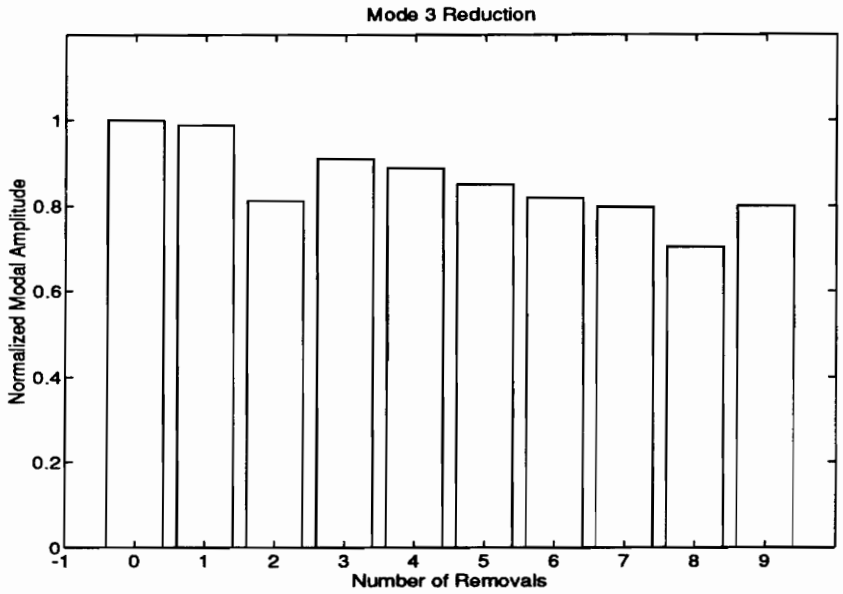

Figure B.2. Normalized Magnitude of the Third Mode of the Piezoelectric Actuator, Cement, Stiffener, Cement, Beam, Attachment Technique

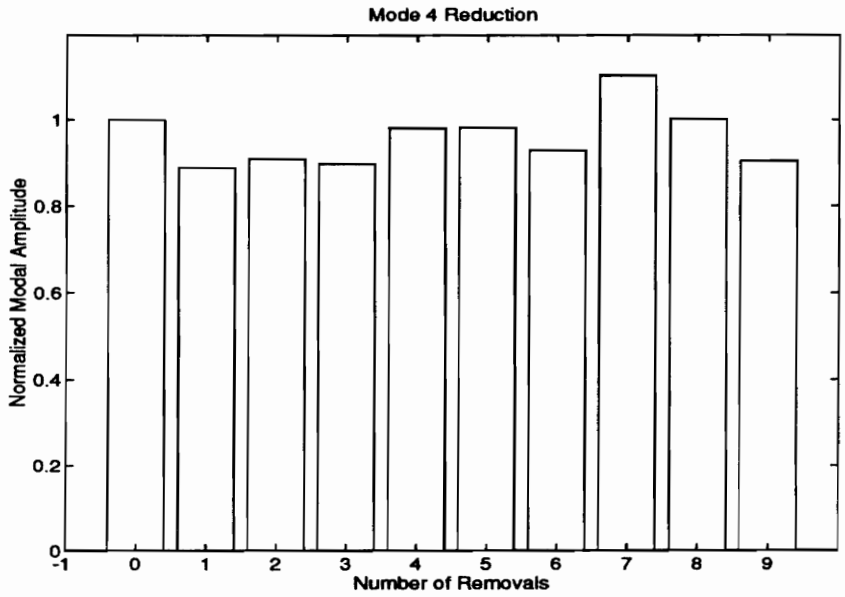

Figure B.3. Normalized Magnitude of the Fourth Mode of the Piezoelectric Actuator, Cement, Stiffener, Cement, Beam, Attachment Technique

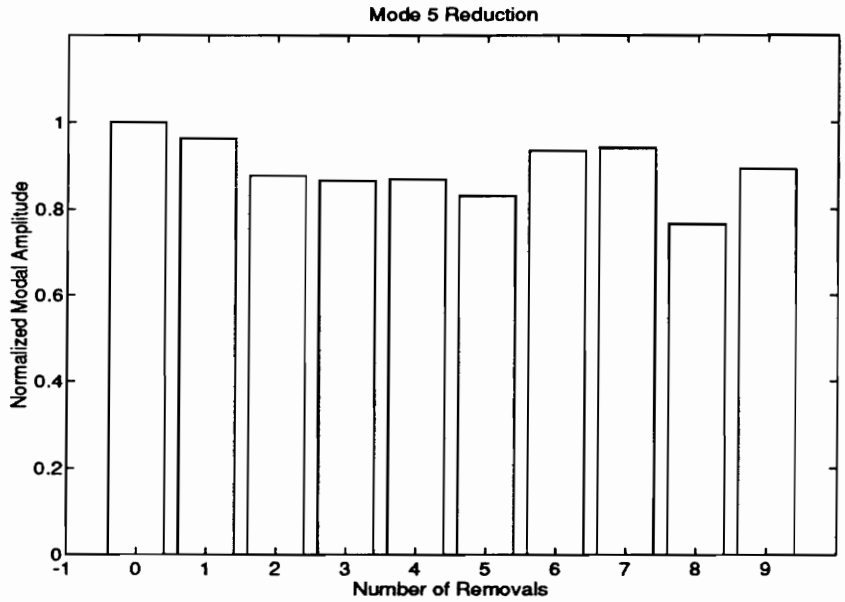

Figure B.4. Normalized Magnitude of the Fifth Mode of the Piezoelectric Actuator, Cement, Stiffener, Cement, Beam, Attachment Technique

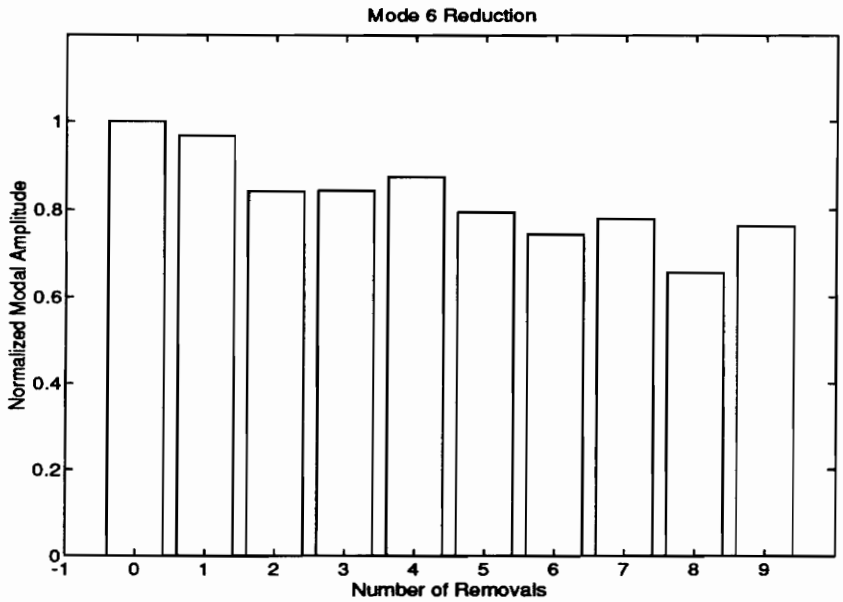

Figure B.5. Normalized Magnitude of the Sixth Mode of the Piezoelectric Actuator, Cement, Stiffener, Cement, Beam, Attachment Technique

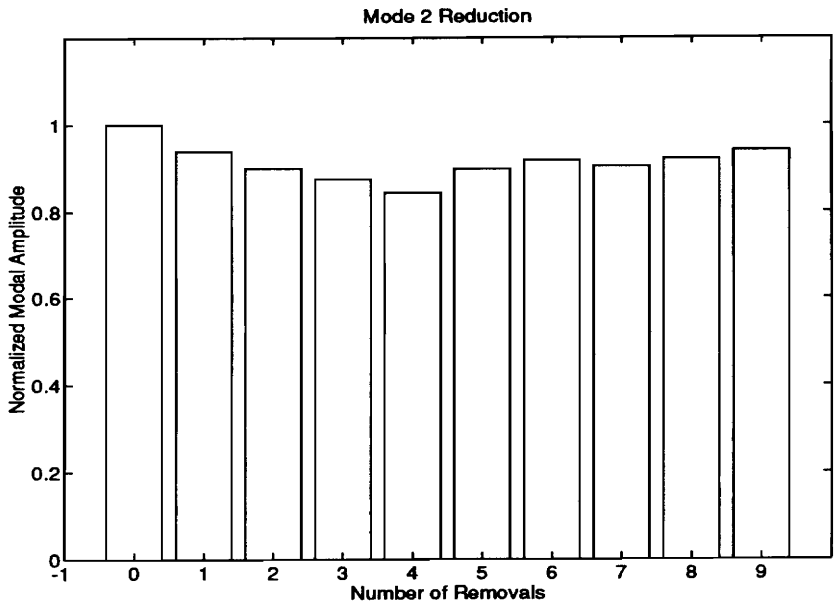

Figure B.6. Normalized Magnitude of the Second Mode of the Piezoelectric Actuator, Wax, Beam, Attachment Technique

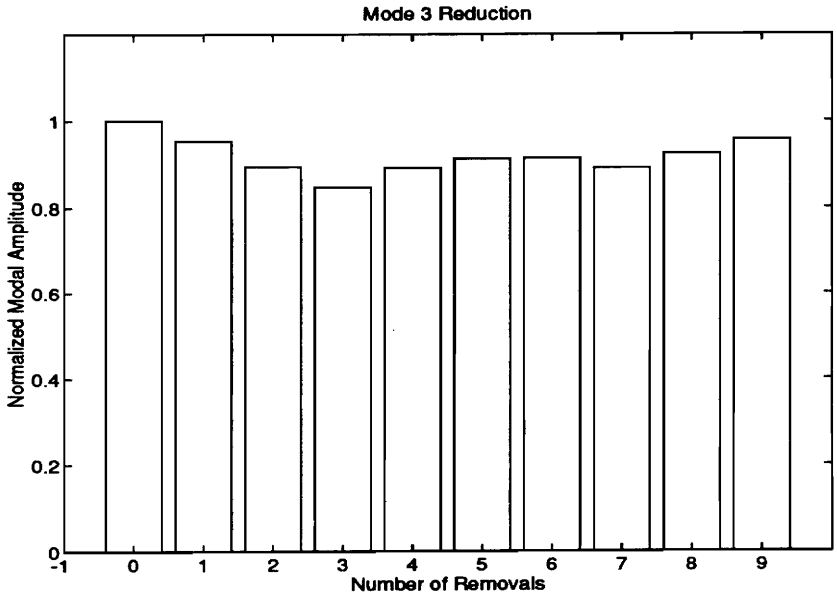

Figure B.7. Normalized Magnitude of the Third Mode of the Piezoelectric Actuator, Wax, Beam, Attachment Technique

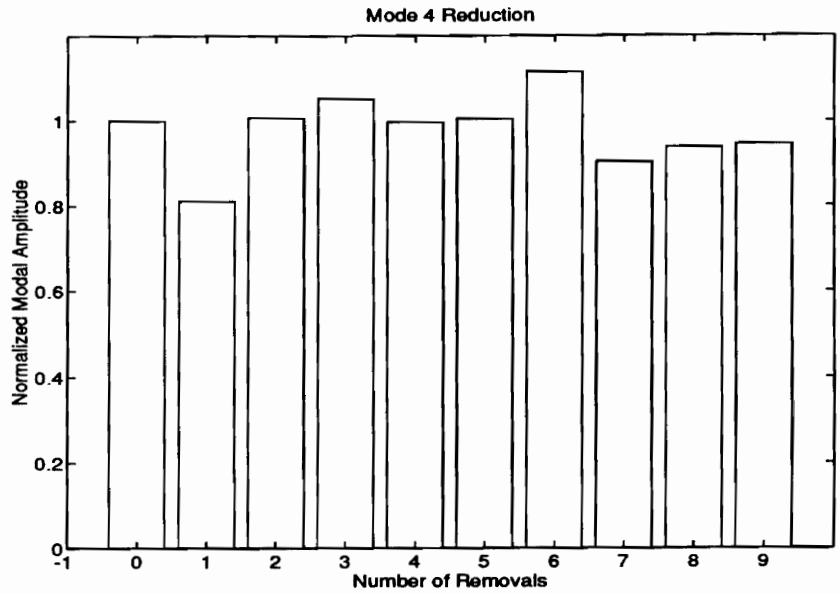

Figure B.8. Normalized Magnitude of the Fourth Mode of the Piezoelectric Actuator, Wax, Beam, Attachment Technique

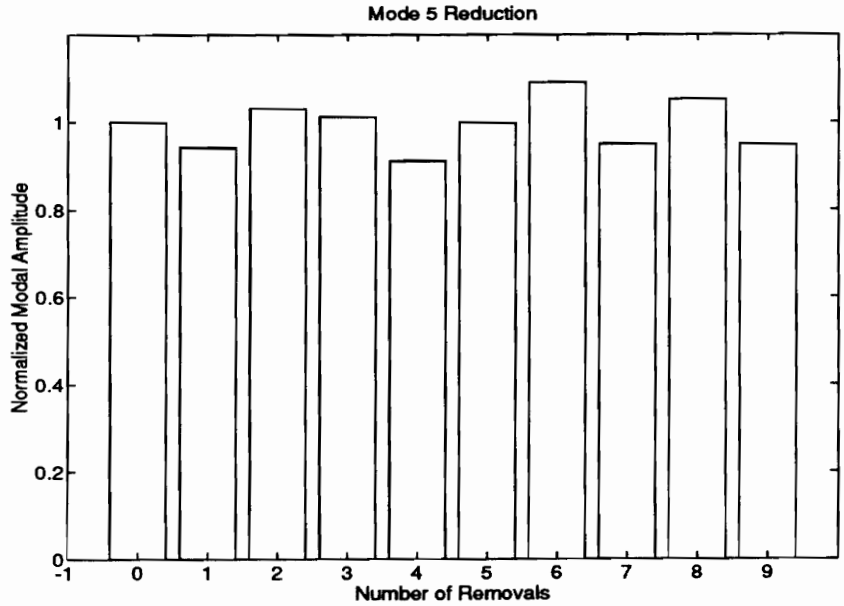

Figure B.9. Normalized Magnitude of the Fifth Mode of the Piezoelectric Actuator, Wax, Beam, Attachment Technique

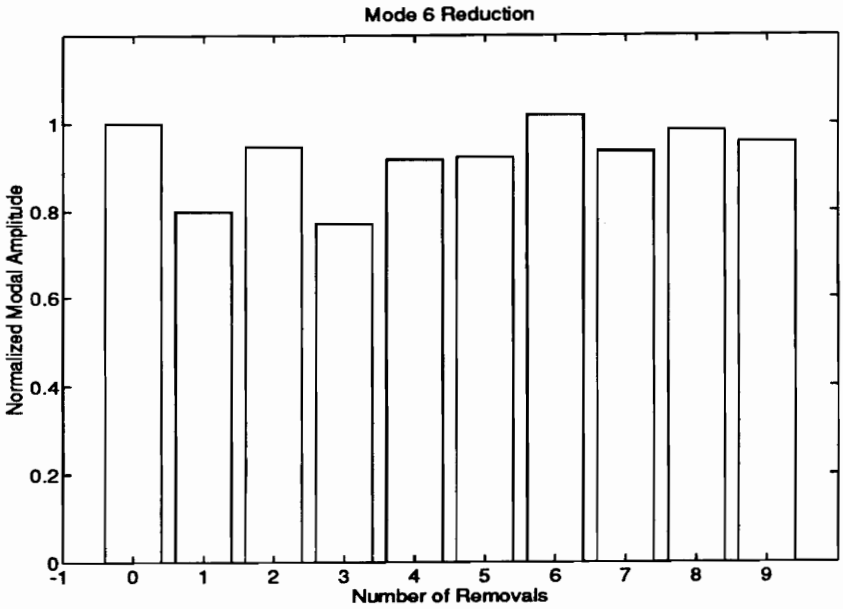

Figure B.10. Normalized Magnitude of the Sixth Mode of the Piezoelectric Actuator, Wax, Beam, Attachment Technique

Vita

Thomas Wade McCray was born on April 29, 1970, in Enid, Oklahoma. He grew up in Richardson, Texas where his parents still reside today. In December of 1992, he completed his Bachelor of Science degree in mechanical engineering from Texas Tech University. While at Texas Tech, he completed an engineering internship with Excel Corporation and was also active outside of academics by serving in leadership positions with the Baptist Student Union.

In January of 1993, he began his graduate studies at Virginia Polytechnic Institute and State University, where he served as a graduate and teaching assistant. Outside academics, he continued active participation in the Virginia Tech Baptist Student Union. Upon graduation, he will begin an engineering career with ITT Automotive in Dayton, Ohio.

Tom W. McCray